Set1-mediated histone H3K4 methylation is required for azole induction of the ergosterol biosynthesis genes and antifungal drug resistance in *Candida glabrata*.

Kortany M. Baker[1], Smriti Hoda[1], Debasmita Saha[1], Livia Georgescu[1], Nina D. Serratore[1*], Yueping Zhang[1*], Nadia A. Lanman[2,3], and Scott D. Briggs[1,2,#]

[1]*Department of Biochemistry,* [2]*Purdue University Center for Cancer Research and* [3]*Department of Comparative Pathobiology, Purdue University, West Lafayette, Indiana 47907*

Running Title: Set1 mediates *ERG* gene induction and drug resistance

Word count of abstract:

[#]To whom correspondence should be addressed: Scott D. Briggs, Department of Biochemistry Hansen Life Science Research Building, 201 S. University Street, West Lafayette, IN 47907, Phone: 765-494-0112, E-mail: sdbriggs@purdue.edu

*Footnote: Current address for Yueping Zhang and Nina Serratore

Nina Serratore: Cook Research Incorporated, 1 Geddes Way, West Lafayette, IN 47906

Yueping Zhang: College of Veterinary Medicine, China Agricultural University, No. 2 Yuanmingyuan West Road, Haidian District, Beijing 100193, China

ABSTRACT

Candida glabrata is an opportunistic pathogen that has developed the ability to adapt and thrive under azole treated conditions. The common mechanisms that can result in *Candida* drug resistance are due to mutations or overexpression of the drug efflux pump or the target of azole drugs, Cdr1 and Erg11, respectively. However, the role of epigenetic histone modifications in azole-induced gene expression and drug resistance are poorly understood in *C. glabrata*. In this study, we show for the first time that Set1 mediates histone H3K4 mono-, di-, and trimethylation in *C. glabrata*. In addition, loss of *SET1* and histone H3K4 methylation results in increased susceptibility to azole drugs in both *C. glabrata* and *S. cerevisiae*. Intriguingly, this increase in susceptibility to azole drugs in strains lacking Set1-mediated histone H3K4 methylation is not due to altered transcript levels of *CDR1*, *PDR1* or Cdr1's ability to efflux drugs. Genome-wide transcript analysis revealed that Set1 is necessary for azole-induced expression of 12 genes involved in the late biosynthesis of ergosterol including *ERG11* and *ERG3*. Importantly, chromatin immunoprecipitation analysis showed that histone H3K4 trimethylation was detected on chromatin of actively transcribed *ERG* genes. Furthermore, H3K4 trimethylation increased upon azole-induced gene expression which was also found to be dependent on the catalytic activity of Set1. Altogether, our findings show that Set1-mediated histone H3K4 methylation governs the intrinsic drug resistant status in *C. glabrata* via epigenetic control of azole-induced *ERG* gene expression.

IMPORTANCE

C. glabrata is the second most commonly isolated species from *Candida* infections, coming in second to *C. albicans*. Treatment of *C. glabrata* infections are difficult due to their natural resistance to antifungal azole drugs and their ability to adapt and become multidrug resistant. In this study, we investigated the contributing cellular factors for controlling drug resistance. We have determined that an epigenetic mechanism governs the expression of genes involved in the late ergosterol biosynthesis pathway, an essential pathway that antifungal drugs target. This epigenetic mechanism involves histone H3K4 methylation catalyzed by the Set1 methyltransferase complex (COMPASS). We also show that Set1-mediated histone H3K4 methylation is needed for expression of specific azole induced genes and azole drug resistance in *C. glabrata*. Identifying epigenetic mechanisms contributing to drug resistance and pathogenesis could provide alternative targets for treating patients with fungal infections.

INTRODUCTION

Candida infections are a major health concern due to the increased frequency of infections and the development of drug resistance (1, 2). Over the years, *Candida glabrata* has become the second most common cause of candidiasis (1-3). In some immunocompromised patients, such as diabetics, patients with hematologic cancer, organ transplant recipients, and the elderly, it is the most predominate *Candida* infection (2-6). The emergence of *C. glabrata* as a major pathogen is likely due to its intrinsic drug resistance to azole antifungal drugs and ability to quickly adapt and acquire clinical drug resistance during treatment (3, 7). The consequence of drug resistance leads to increases in healthcare costs as well as lower success rates in treatment and an increase in mortality (8-10).

C. glabrata naturally has low susceptibility to azole drugs and because of this attribute, echinocandins are the preferred drug choice for treating *C. glabrata* infections (11). *C. glabrata* can also acquire clinical resistance to azole drugs which is often due to overexpressing the ABC-transporter drug efflux pump Cdr1 or Pdh1 (Cdr2) caused by gain of function mutations in the transcription factor Pdr1 (7, 12-14). In other *Candida* species, acquired clinical azole resistance can also be due to overexpression of *ERG11* due to gain of function mutations in the Upc2 transcription factor or mutations in *ERG11* (15-17). However, for unbeknownst reasons, *ERG11* or *UPC2* mutations are typically not found in clinically drug resistant *C. glabrata* strains (7, 18-20).

Because pathogenic fungi can rapidly adapt to various cellular environments and xenobiotic drug exposures, epigenetic mechanisms are also likely contributing to altered gene expression profiles permissive for adaptation and drug resistance. Several studies

in *C. albicans* support this hypothesis and show that epigenetic factors such as histone acetyltransferases, *Ca*Gcn5 and *Ca*Rtt109, and histone deacetylases, *Ca*Rpd3 and *Ca*Hda1 are important for either fungal pathogenesis and/or drug resistance (21-25). In contrast, epigenetic factors that post-translationally modify histones have not been extensively studied for their roles in drug resistance in *C. glabrata*. Nonetheless, Orta-Zavalz et al., have shown that deleting histone deacetylase, *CgHST1* decreases susceptibility to fluconazole which is likely attributed to an increase in transcript levels of *CgPDR1* and *CgCDR1* under untreated conditions (26). In addition, a recent publication by Filler et al., has indicated that *C. glabrata* strains that are deleted for *GCN5*, *RPD3*, or *SPP1* have increased susceptibility to caspofungin when using high concentrations (27). However, no mechanistic understanding such as gene targets or changes in chromatin/histone modifications was provided for the caspofungin hypersensitive phenotype.

Previous publications from our lab demonstrated that in *S. cerevisiae* loss of Set1, a known histone H3K4 methyltransferase, has a hypersensitive growth defect in the presence of the antifungal metabolite, brefeldin A (BFA) and clinically used azole drugs (28, 29). We determined that hypersensitivity to BFA was due to a decrease in ergosterol levels in *S. cerevisiae* strains lacking histone H3K4 methylation. However, until this study, no mechanistic understanding has been provided why a strain lacking *SET1* alters azole drug susceptibility. Furthermore, in *C. albicans*, loss of *SET1* appears to alter virulence but not azole drug resistance (30). To determine if an increase in azole susceptibility is conserved in a human fungal pathogen closely related to *S. cerevisiae*,

we investigated the role of Set1 and its mechanistic contribution to drug resistance in *C. glabrata*.

In this study, we show for the first time that Set1-mediates histone H3K4 mono-, di-, and trimethylation in *C. glabrata* and loss of Set1-mediated histone H3K4 methylation alters the azole drug susceptibility of *C. glabrata* similar to what is seen in *S. cerevisiae*. This increase in susceptibility to azole drugs in *C. glabrata* strains lacking Set1-mediated histone H3K4 methylation is not a consequence of altered expression levels of *CDR1*, *PDR1* or their ability to efflux drugs. Interestingly, RNA-sequencing (RNA-seq) revealed that Set1 is required for azole-induced expression of *ERG* genes, including *ERG11* and *ERG3.* This azole-induced gene expression was dependent on Set1 methyltransferase activity and associated with gene-specific increases in histone H3K4 trimethylation on *ERG11* and *ERG3* chromatin. Overall, we have provided a mechanistic understanding of why Set1 mediated histone H3K4 methylation governs the intrinsic drug resistant status in *C. glabrata.* Identifying and understanding the epigenetic mechanisms contributing to drug resistance will be important for the development of alternative drug targets for treating patients with fungal infections.

RESULTS

Loss of Set1-mediated histone H3K4 methylation in *S. cerevisiae* and *C. glabrata* alters azole drug efficacy. Set1 is a known SET domain-containing lysine histone methyltransferase that is conserved from yeast to humans and the enzymatic activity of the SET domain catalyzes mono-, di-, and trimethylation on histone H3 at Lysine 4 (Lys4) (31, 32). Our previous work in *Saccharomyces cerevisiae* (*S. cerevisiae*) has determined that loss of *SET1* in the BY4741 background strain results in increased susceptibility to azole drugs suggesting that H3K4 methylation is necessary for mediating wild-type azole drug resistance. To determine the role of histone H3K4 methylation in azole drug efficacy, we constructed histone H3K4R mutations in the BY4741 background strain. Because *S. cerevisiae* has two genes encoding histone H3, two yeast strains were constructed where a histone H3K4R mutation was integrated at one histone H3 gene keeping the other gene wild-type (ScH3K4R-1) while the other strain contained H3K4R mutations integrated at both histone H3 genes (ScH3K4R-2, see supplemental table S1). To determine if loss of histone H3K4 methylation altered azole drug sensitivity similar to a *set1Δ* (Sc*set1Δ*) strain, a serial-dilution spot assay was performed. Both Sc*set1Δ* and *Sc*H3K4R mutant strains were grown in synthetic complete minimal media and spotted on SC agar plates with and without 8 µg/mL fluconazole (Fig. 1A). These data show that loss of histone H3 methylation by deleting Sc*SET1* or mutating histone H3 where both histone H3 genes are mutated at K4 (ScH3K4R-2), resulted in similar azole drug hypersensitivity when compared to each other (Fig. 1A). To confirm that histone H3K4 methylation was abolished in these strains, western blot analysis was performed using methyl-specific antibodies to detect

histone H3K4 mono-, di-, and trimethylation (Fig. 1B). Histone H3 was used for a loading control (Fig. 1B). As expected, histone methylation was abolished in ***set1Δ*** and in H3K4R-2 mutation strains but not in the histone H3K4R-1 strain (Fig. 1B). Together our data demonstrate that the presence of Histone H3K4 methylation is critical for maintaining wild-type azole drug susceptibility.

To determine if an azole hypersensitive growth phenotype observed in *S. cerevisiae* is also conserved in the human fungal pathogen *C. glabrata*, WT (*Cg*WT) and a ***set1***Δ (*Cgset1*Δ) strain were spotted on SC agar plates with and without 16 µg/mL fluconazole (Fig. 1C). Similar to what was observed in *S. cerevisiae*, deleting *SET1* in *C. glabrata* 2001 (CBS138, ATCC2001) showed an increase in azole susceptibility when compared to a *Cg*WT strain (Fig. 1C). Additionally, the *Cgset1Δ* strain had a significant growth delay in liquid growth cultures comparted to *Cg*WT when treated with 32 µg/mL fluconazole (Fig. 1E). Western blot analysis showed that deleting *CgSET1* abolished all histone H3K4 mono-, di-, and trimethylation confirming that *CgSET*1 is the sole histone H3K4 methyltransferase in *C. glabrata* (Fig. 1D). Altogether, our results show Set1-mediated histone H3K4 methylation in *S. cerevi*siae and *C. glabrata* is conserved and is necessary for maintaining a wild-type resistance to azole drugs.

Loss of *C. glabrata* Set1 complex members alters azole efficacy and histone H3K4 methylation. In *S. cerevisiae*, Set1 forms a complex referred to as the Complex Proteins Associated with Set1 or COMPASS. COMPASS forms a stable complex with 8 proteins which includes the catalytic subunit Set1, Swd1, Swd2, Swd3, Spp1, Bre2, Sdc1, and Shg1 (33-35). Previous studies in *S. cerevisiae* have determined that Swd1, Swd2, Swd3, Spp1, Bre2, and Sdc1 are necessary for Set1 to properly catalyze the

various states of histone H3K4 mono-, di, and trimethylation (33-38) . To determine if COMPASS components are required to govern azole drug efficacy and Set1-mediated histone H3K4 methylation in *C. glabrata*, we generated deletion strains lacking *SET1*, *SPP1*, *BRE2* and *SWD1* and determined their MIC in RPMI media (Fig. 2A). Consistent with our agar and liquid growth assays in Figure 1, the *Cgset1Δ* strain showed increased susceptibility to fluconazole with an 8-fold difference in MIC compared to the *Cg*WT strain (Fig. 2A). A *Cgswd1Δ* strain showed a similar MIC as the *Cgset1Δ* strain while the MIC of *Cgspp1Δ* and *Cgbre2Δ* deletion strains were 4-fold different than the WT strain (Fig 2A). Furthermore, all *C. glabrata* COMPASS deletions strains showed an increase in susceptibility to azole drugs on agar plates similar to *S. cerevisiae* COMPASS deletion strains except for the *Scspp1Δ* which is likely due to differences in the histone H3K4 methylation status (Fig. 2B, 2C, S1A, and (29, 33, 34, 36, 38).

Western blot analysis determined that *Cgswd1Δ* strain lacked all forms of histone H3K4 methylation (Fig. 2C) which is also observed in *Cgset1Δ* and *Scset1Δ* strains (Fig. 2C and 1D). In contrast, deletion of *CgSPP1* and *CgBRE2* abolished all detectable levels of H3K4 trimethylation and significantly reduced the levels of histone H3K4 mono- and dimethylation. Taken together, our data show that when *C. glabrata* COMPASS subunits *SET1* and *SWD1* are deleted, global loss of histone H3K4 methylation is observed similar to what is seen when the subunits are deleted in *S. cerevisiae* (Fig 2C and (33, 34, 36, 38). However, the *Cgspp1Δ* has a total loss of histone H3K4 trimethylation and significant loss of histone H3K4 mono-and dimethylation similar to the *Cgbre2Δ* and *Scbre2Δ* strains (Fig 2C). For unknown reasons, the pattern of histone H3K4 methylation is different in the *Scspp1Δ* strain which only has a reduction in

histone H3K4 trimethylation but not mono- or dimethylation (33-39). Altogether, these results suggest that the COMPASS complex is needed to mediate proper histone H3K4 methylation and WT resistance to azole drugs.

The methyltransferase activity of Set1 governs azole drug efficacy in *C. glabrata*. To confirm that altered azole efficacy in the *Cgset1Δ* strain was due to loss of *SET1* and not a secondary mutation, a genomic fragment containing the *CgSET1* promoter, 5'UTR, open reading frame, and 3'UTR was amplified by PCR and cloned into the *C. glabrata* plasmid, pGRB2.0 (40). Because a H1017K mutation in the SET domain of *S. cerevisiae* Set1 is known to be catalytically inactive (28, 41, 42), we performed site-directed mutagenesis on pGRB2.0-*CgSET1* and generated an analogous mutation in *C. glabrata* Set1 at H1048K determined using the sequence alignment in Fig. 3A. Additionally, we deleted *SET1* in *C. glabrata* 2001HTU (ATCC200989) to utilize the *ura3* auxotrophic marker (43). Importantly, *Cg*2001HTU lacking *SET1* was hypersensitive to azole drugs similar to when *SET1* was deleted in *Cg*2001 (Fig. 1C and 3B). Furthermore, transformation of pGRB2.0-*CgSET1* into the *Cg*2001HTU/*set1Δ* strain was able to rescue azole hypersensitivity while pGRB2.0-*Cgset1H1048K* did not rescue wild-type azole drug resistance as shown by serial dilution spot assays grown on SC agar plates with 32 µg/mL fluconazole (Fig. 3B). MIC assays under SC-ura conditions also show similar results (see Supplemental Fig. S1B). Western blot analysis indicated that pGRB2.0-*CgSET1* expression in *Cg*2001HTU/*set1Δ* strain restored histone H3K4 methylation to wild-type levels while *Cgset1H1048K* did not rescue histone H3K4 methylation confirming that this mutation lacks catalytic activity similar to *Scset1H1017K* (Fig. 3C). Importantly, quantitative real-time PCR analysis (qRT-PCR) confirmed that

the plasmids expressing *CgSET1* and *Cgset1H1048K* were similar to the endogenously expressed *SET1* (Fig. S1C). This shows that loss of histone H3K4 methylation was not due to difference in expression levels but due to the catalytic inactivation of *Cgset1H1048K*. These data suggest that altered azole drug efficacy in *Cgset1Δ* strains are specifically due to the loss of *SET1* and its catalytic activity.

Drug efflux pump expression and function is not altered in a *C. glabrata set1*Δ strain. In *Candida glabrata*, the major mechanisms for changes in drug resistance are due to changes in expression of *CDR1*, the main drug efflux pump, or gain-of-function mutations in *PDR1*, a gene that encodes the transcription factor for *CDR1* (7, 12, 19, 20, 44). To determine if altered drug resistance in *Cgset1Δ* cells was due to changes in *CDR1* or *PDR1* expression, we analyzed the transcript levels of *CDR1* and *PDR1* via qRT-PCR (Fig. 4A and B). We observed that *Cgset1Δ* cells grown with and without azoles do not significantly affect transcript levels of *CDR1* or *PDR1* when compared to a wild-type strain (Fig. 4A and B). Additionally, we analyzed the transcript levels of transporters *SNQ2, YOR1,* and *PDH1.* We did not see any significant changes in *SNQ2* or *YOR1,* but we did see a decrease in *PDH1* transcripts in a *set1Δ* strain upon azole treatment (Fig. S2). However, previous studies have shown loss of *PDH1* alone is not sufficient to lead to azole sensitivity (45). To determine if drug efflux was functional in *Cgset1Δ* cells, a Nile Red fluorescence-based assay was performed. Nile Red, a fluorescent lipophilic stain, has been shown to be a substrate for the ABC transporter Cdr1 in *C. albicans* and *C. glabrata* (46, 47). As a control, we also generated a *Cgpdr1*Δ strain, a deletion strain known to disrupt the expression of *CDR1* and subsequently prevent drug or Nile Red efflux (15). The Nile Red assay showed that *Cgset1Δ* cells had

246 similar levels of Nile Red as wild-type cells but less Nile Red than *Cgpdr1Δ* cells (Fig.
247 4C). To induce *CDR1* expression levels, *Cgset1Δ* and wild-type cells were treated with
248 fluconazole. Although azole treatment did reduce the amount of Nile Red in *Cgset1Δ*
249 and wild-type cells compared to untreated cells, there was no discernable differences
250 observed between *Cgset1Δ* and wild-type cells for their ability to efflux Nile Red, (Fig.
251 4C). Altogether these data suggest that cells lacking *SET1* have similar efflux
252 capabilities as wild-type cells in the presence or absence of azole treatment. This
253 suggests that the increase in azole sensitivity seen in a *Cgset1*Δ strain is not due to
254 malfunction of Cdr1 expression or its efflux capabilities.

255 **Loss of Set1 leads to decreased expression of genes involved in the sterol**
256 **biosynthesis pathway when treated with fluconazole.** Because drug efflux function
257 or transcript levels was not disrupted in a *Cgset1*Δ strain, we used RNA-sequencing
258 analysis to provide insight into what gene pathway might be disrupted in the *Cgset1*Δ
259 strain and explain why a loss of *SET1* alters azole drug efficacy. *Cg*WT and *Cgset1*Δ
260 strains were treated with 64 µg/mL fluconazole for three hours in SC complete media
261 and RNA was extracted for RNA-sequencing. Principle component analysis (PCA) and
262 differentially expressed genes (DEG) analysis demonstrated by the volcano scatter plot
263 ($-\log_2$ false discovery rate (FDR), y-axis) versus the fold change (x- axis) of the DEGs)
264 indicate that the untreated and treated *Cg*WT strain is substantially and statistically
265 different from the untreated and treated *Cgset1*Δ (Fig 5). DESeq2 analysis was used to
266 identify the differentially expressed genes (DEGs) under fluconazole treatment using an
267 FDR of 0.05. From this analysis, a total of 2389 genes were differentially expressed in
268 *Cgset1*Δ vs. *Cg*WT under untreated condition (Fig. 5B). Whereas, 1508 genes were

differentially expressed under treated conditions, where we observed 800 (14.2%) genes that were upregulated and 708 (12.6%) genes that were downregulated out of 5615 genes in *Cgset1Δ* compared to *Cg*WT (Fig. 5C and supplemental data). After applying a 1.4-fold cutoff to the data, we observed 1,644 genes differentially expressed in the untreated *Cgset1*Δ vs. *Cg*WT strains. In the treated strains, with a 1.4-fold cutoff, we observed 543 (9.7%) genes were down in a *Cgset1Δ* vs CgWT and 626 (11.1%) genes were up. These data show that *SET1* is important for maintaining proper gene expression in *C. glabrata*.

Because Set1-mediated histone H3K4 methylation is known to play a key role in gene activation, we focused our attention on genes downregulated in *Cgset1Δ* compared to *Cg*WT. For azole-treated strains. GO Term Finder of the gene sets that were downregulated found significant GO terms involved in lipid, steroid and sterol/ergosterol metabolism or biosynthesis (Fig. 5D). For untreated strains, GO Term Finder identified significant GO terms involved in lipid metabolism but not steroid and sterol/ergosterol metabolism or biosynthesis (supplemental table S6). Interestingly, our data showed that 12 of the 12 genes involved in the late ergosterol biosynthesis pathway are down 1.4-fold or more in a *Cgset1Δ* compared to *Cg*WT under azole treated conditions (Fig. 5C, S4A & B and supplemental table S7). Whereas, 5 of the 12 late pathway *ERG* enzyme encoding genes were down in a *Cgset1Δ* compared to *Cg*WT under untreated conditions using a 1.4-fold difference in gene expression as a cutoff (Fig. 5D. and Supplemental table S7). Two of these differentially expressed genes *ERG11,* the gene that encodes the target of azoles, and *ERG3*, the gene that encodes the enzyme responsible for production of a toxic sterol when cells are treated with

azoles, are known to play roles in azole drug resistance in various *Candida* species (17, 19, 48-50). To validate results seen in RNA-sequencing analysis, *ERG11* and *ERG3* transcript levels were analyzed by qRT-PCR. Our analysis showed that upon azole treatment, *ERG3* and *ERG11* transcript levels are induced in a WT strain (Fig. 5C and D) while loss of *SET1* prevented WT induction of both *ERG11* and *ERG3* under azole conditions. Even though our untreated RNA sequencing data set did show minor changes in *ERG3* and *ERG11* transcript levels, we did not detect any significant changes between *Cgset1Δ* and *Cg*WT cells when grown under untreated standard log-phase conditions using qRT-PCR analysis (Fig. 5E and F). We also performed gene expression analysis to determine if *ERG* gene transcript induction still depended on Set1 in saturated cultures. We show in both exponential and saturated cultures Set1 is necessary for *ERG3* and *ERG11* induction upon azole treatment in *C. glabrata* (Fig. 5E&F and S3A&B). Because *ERG3* transcript levels were decreased, we do not anticipate azole sensitivity is due to an increase in toxic sterols but by the lack of induction of *ERG11* and other *ERG* genes resulting in lower total cellular ergosterol levels (51, 52).

Set1-mediated histone H3K4 methylation is enriched on *ERG* gene chromatin and is required for azole induction of *ERG* genes. Because histone H3K4 trimethylation is associated with gene induction, we wanted to determine if Set1 was directly catalyzing histone H3K4 methylation on chromatin at *ERG* loci. To determine if histone H3K4 trimethylation was present at *ERG11* and *ERG3* chromatin, chromatin immunoprecipitation (ChIP) analysis was performed using histone H3K4 trimethyl-specific antibodies. As expected, histone H3K4 trimethylation is highly

315 enriched at the 5'-ends of the open reading frame of *ERG11* and *ERG3* in untreated
316 conditions and further enriched upon azole treatment corresponding to increased
317 transcript levels of *ERG11* and *ERG3* in both exponential and saturated cell cultures
318 (Fig. 6A & B and S3D & E).

319 To confirm that this was due to the methyltransferase activity of Set1, we
320 performed qRT-PCR transcript analysis using the *Cg*2001HTU*set1Δ* strain expressing
321 pGRB2.0 only, pGRB2.0-*CgSET1*, and pGRB2.0-*Cgset1H1048K*. *Cg*2001HTU
322 expressing pGRB2.0 only was used as our WT control. As shown in Figure 6C and D,
323 pGRB2.0-*CgSET1* was able to induce *ERG11* and *ERG3* similar to WT cells under
324 azole treatment indicating that *SET1* expression could rescue the *ERG* gene expression
325 in the *Cg*2001HTU*set1Δ* strain. This rescue of *ERG* gene expression was dependent on
326 the catalytic activity of Set1 since expression of pGRB2.0-*Cgset1H1048K* did not
327 restore *ERG* gene expression under azole treatment. Additionally, it looked similar to
328 the *Cg*2001HTU*set1Δ* strain expressing pGRB2.0 indicating that the catalytic activity of
329 Set1 is required for azole gene induction. Altogether, these data show that Set1-
330 mediated histone H3K4 methylation directly targets the chromatin of *ERG* genes, and
331 this epigenetic modification is required for azole induction of *ERG* genes. Based on our
332 results, the lack of Set1 or histone H3K4 methylation on *ERG11* chromatin prevents the
333 transcriptional response for inducing *ERG* genes which consequently disrupts
334 ergosterol homeostasis, thus making the *Cgset1Δ* strains more susceptible to azole
335 drugs.

336

337

DISCUSSION

In this study, we established that loss of Set1-mediated histone H3K4 methylation alters azole drug susceptibility in *S. cerevisiae* and *C. glabrata*. This increase in susceptibility to azole drugs in a *Cgset1Δ* strain was not because of the typical changes in *CDR1* and *PDR1* expression levels or their ability to efflux drugs. However, we observed that strains lacking histone H3K4 methylation failed to induce *ERG* genes. This azole-induced gene expression was dependent on Set1 methyltransferase activity and correlated with gene-specific increases in histone H3K4 trimethylation on chromatin at *ERG* genes (see model, Fig. 7). Overall, we have provided an epigenetic mechanism upon azole treatment that is dependent on histone H3K4 methylation governing ergosterol homeostasis. Identifying and understanding this Set1-*ERG* pathway and other epigenetic mechanisms contributing to altered drug susceptibility will be important for the development of alternative drug targets that could be used in combinatorial therapy for treating patients with drug resistant fungal infections.

Set1 is the catalytic subunit of a multi-subunit protein complex called COMPASS that mono-, di-, and trimethylates histone H3K4. In this study, we show that *C. glabrata* Set1 is the sole histone H3K4 methyltransferase under log-phase growth conditions since deletion of *SET1* abolishes all forms of histone H3K4 methylation similar to what is seen in *S. cerevisiae* and *C. albicans*. Deletion of the genes encoding *C. glabrata* COMPASS complex subunits Swd1 and Bre2 have similar loss of histone H3K4 methylation as their *S. cerevisiae* counterparts (see Fig 2C and (33, 34, 36, 38)). However, deleting *SPP1* in *C. glabrata* abolishes all histone H3K4 trimethylation and

significantly reduces the levels of histone H3K4 mono- and dimethylation which is in contrast to what is found in a *Scspp1Δ* strain where only histone H3K4 trimethylation is disrupted but retains WT levels of mono- and dimethylation (33, 34, 36, 38). We speculate that this difference in histone H3K4 methylation pattern is due to how *Cg*Spp1 assembles with the COMPASS complex allowing *Cg*Spp1 to have a greater impact on the overall catalytic activity of COMPASS. Interestingly, this pattern of methylation appears to correlate with sensitivity to azole drugs (compare Fig. 2B with supplemental Fig. S1A) where *Scspp1Δ* grows more similar to a WT strain than *Cgspp1Δ* when grown on azole containing plates.

Our published observation and current data show that loss of *SET1* alters ergosterol homeostasis and azole susceptibility in *S. cerevisiae* and *C. glabrata* (28, 29). Specifically, loss of *SET1* in *S. cerevisiae* altered expression of genes involved in ergosterol biosynthesis under untreated conditions (28). In contrast, in *C. glabrata*, significant changes in *ERG* gene expression were only observed under azole treated conditions but not untreated conditions suggesting that histone H3K4 methylation is needed for azole induced gene induction and not basal level expression (Fig. 5E and F). Although regulation of ergosterol biosynthesis has been shown to be coupled to expression of ABC transport genes such as *CDR1* and its transcription factor Pdr1 (53, 54), compensatory changes in *CDR1 and PDR1* expression levels was not observed in a *cgset1Δ* strain when treated with azole drugs (Fig. 4A and 4B). More investigation will be needed to understand how *CDR1* and/or *PDR1* are epigenetically regulated in *C. glabrata* (26, 55).

In *C. albicans*, Raman et al., reported that loss of *SET1* in did not alter azole sensitivity but did decrease virulence in mice (30). Furthermore, *C. albicans* is naturally more susceptible to azole drugs than *S. cerevisiae* and *C. glabrata*. We suspect the difference observed in these organisms in azole sensitivity and gene regulation is likely due to their differences in sterol uptake. For example, *C. glabrata and S. cerevisiae* can uptake sterols under a variety of conditions where *C. albicans* does not (56). Interestingly, loss of *SET1* in *S. cerevisiae* can also permit sterol uptake under aerobic conditions since sterol transporter transcripts of *PDR11* and *AUS1* are increased in a *Scset1Δ* strain (28). In contrast, *AUS1,* is constitutively expressed in *C. glabrata* under aerobic and anaerobic conditions allowing sterol uptake. Even though *AUS1* is constitutively expressed, we do observe a slight increase in *AUS1* transcript levels in a *Cgset1Δ* relative to *Cg*WT under untreated conditions but not treated conditions (see supplemental data Fig. S3C). Alternatively, loss of *SET1* may not alter azole efficacy in *C. albicans* because it does not regulate the expression of *ERG* genes or sterol transporters. However, other epigenetic factors as indicated below are likely playing a role in *C. albicans*. Nonetheless, additional studies will be needed to determine the precise mechanistic cause of these distinct differences.

Overall, our data suggest that histone H3K4 methylation is an epigenetic mechanism to help induce *ERG* gene expression when *C. glabrata* strains are exposed to azole drugs. We propose histone H3K4 methylation and possibly other epigenetic marks are contributing factors to *C. glabrata's* natural resistance to azole drugs. Interestingly, several histone deacetylases (HDACs) have been implemented in azole resistance in *C. albicans* such as *Ca*Hda1, *Ca*Rpd3, and *Ca*Hos2 (22, 23, 57-59).

406 Additionally, HDAC inhibitors have been shown to have a synergistic effect on cells
407 when combined with azoles and echinocandins (57, 58, 60, 61). Interestingly, the
408 treatment of *C. albicans* with trichostatin A (TSA) lacks the trailing effect observed in
409 MIC assays when using azole drugs and the lack of trailing effect was attributed to
410 reduced *CDR* and *ERG* gene expression (58, 62). In a similar manner, *Cgset1Δ* also
411 lacks a trailing effect in our MIC assays (personal observation) which we suspect is
412 specifically due to the lack of azole-induced *ERG* gene expression since *CDR1*
413 expression was not altered (Fig. 4A and 5). Furthermore, treatment of drug resistant
414 fungal pathogens including various isolates of *C. glabrata* with a Hos2 inhibitor
415 MGCD290 showed synergy with azole drugs which converted the MICs of azole
416 treatment from resistant to susceptible (60). Since Hos2 is known to be a key
417 component of the Set3 complex and the Set3 complex is recruited to chromatin via
418 Set1-mediated histone H3K4 methylation (63, 64), it is likely MGCD290 is mediating its
419 effect with azoles through inhibiting azole-induced *ERG* gene expression.
420 We expect that the Set1-*ERG* regulatory pathway controlling ergosterol
421 homeostasis will not only impact drug resistance but will also impact fungal
422 pathogenesis. For example, *C. albicans* strains lacking *ERG11* or *ERG3* produces
423 avirulent hyphae, decreases the adherence to epithelial cells, and reduces virulence of
424 *C. albicans* in oral mucosal infections and disseminated candidiasis (65-67). Similarly,
425 deletion of *SET1* in *C. albicans* also forms hyphae, decreases epithelial adherence, and
426 reduces virulence of *C. albicans* in disseminated candidiasis (30). Based on our current
427 data in *C. glabrata*, we speculate that loss of *SET1* in *C. albicans* reduces expression of
428 *ERG* genes and ergosterol production which in turn reduces epithelial adherence and

thus alters the virulence of *C. albicans*. Therefore, the loss of *SET1* could also alter the virulence of *C. glabrata*. Interestingly, several genes encoding cell wall proteins and adhesion factors are also down regulated in a *Cgset1Δ* strain as determined by RNA-sequencing. However, future studies will be needed to determine if this Set1-*ERG* regulatory pathway exists for *C. albicans* and if *SET1* is controlling virulence factors for *C. glabrata*.

Overall, the occurrence of multidrug resistant strains is increasing across all *Candida* species. In addition, with the development and identification of multidrug resistant fungal species such as *C. auris*, a pathogen of urgent concern for the CDC, it is imperative to find alternative treatment options. Our study along with others provide compelling evidence that epigenetic modifiers are playing key roles in fungal pathogenesis and drug resistance. Understanding these epigenetic events and the pathways they impact are needed to develop new drug therapies so that current and newly emerging multidrug resistant fungal pathogens can be effectively treated.

MATERIALS AND METHODS

Plasmids and yeast strains

All plasmids and yeast strains are described in Table S1 and S2. *C. glabrata* 2001 (CBS138, ATCC2001) and *C. glabrata* 2001HTU (ATCC200989) were purchased from ATCC (43). A genomic fragment containing the *CgSET1* promoter, 5'UTR, open reading frame, and 3'UTR was amplified by PCR and cloned into the pGRB2.0 plasmid. The pGRB2.0 plasmid was purchased from Addgene. Standard, site-directed mutagenesis was used to generate *Cgset1H1048K*. *Candida glabrata SET1*, *BRE2*, *SWD1*, *SPP1*, and *PDR1* genes were deleted via standard homologous recombination. Briefly, drug

452 resistant selection markers were PCR amplified with Ultramer DNA Oligos (IDT) using
453 pAG32-HPHMX6 (hygromycin) or pAG25-NATMX6 (nourseothricin).

454 **Serial dilution spot and liquid growth assays**

455 For serial dilution spot assays, yeast strains were inoculated in SC media and grown to
456 saturation overnight. Yeast strains were diluted to an OD_{600} of 0.1 and grown in SC
457 media to log phase shaking at 30°. The indicated strains were spotted in five-fold
458 dilutions starting at an OD_{600} of 0.01 on untreated SC plates or plates containing 16,32,
459 or 64 µg/ml fluconazole (Sigma-Aldrich, St. Louis, MO). Plates were grown at 30° for 1-3
460 days. For growth assays, the indicated yeast strains were inoculated in SC media and
461 grown to saturation overnight. Yeast strains were diluted to an OD_{600} of 0.1 and grown
462 in SC media to log phase shaking at 30°. The indicated strains were diluted to an OD_{600}
463 of 0.0001 in 100 µl SC media. Cells were left untreated or treated with 64 µg/ml
464 fluconazole and grown for 50 hrs shaking at 30°. The cell density OD_{600} was determined
465 every 1 hr using the Bio-Tek Synergy 4 multimode plate reader.

466 **Cell extract and Western blot analysis**

467 Whole cell extraction and western blot analysis to detect histone modifications were
468 performed as previously described (36, 68). The histone H3K4 methylation-specific
469 antibodies were used as previously described; H3K4me1(Upstate 07-436, 1:2,500),
470 H3K4me2 (Upstate 07-030, 1:10,000), H3K4me3 (Active motif 39159, 1:100,000) (28,
471 69). Histone H3 antibodies were used as our loading control (Abcam ab1791, 1:10,000).

472 **RNA-sequencing analysis**

473 The CBS138 *Cg*2001 WT and *set1*Δ strains were inoculated in SC media and grown to
474 saturation overnight. Cells were diluted to an OD_{600} of 0.1 and recovered to log phase

for 3 hours shaking at 30°. Prior to treatment, cells were collected for the untreated sample and zero time point. Cultures were treated at an OD_{600} of 0.2 with 64 µg/ml fluconazole (Sigma-Aldrich, St. Louis, MO) dissolved in DMSO as previously described (70). Cells were collected after 3 hours. Total RNA of three biological replicates for each condition and sample were isolated by standard acid phenol purification, treated with DNase (Ambion), and total RNA was purified using standard acid phenol purification. The quality of the RNA was tested using an Agilent Bioanalyzer 2100 using the High Sensitivity DNA Chip. The complementary DNA library was prepared by the Purdue Genomics Facility using the TruSeq Stranded Kit with poly(A) selection (Illumina) according to the manufacturer's instructions. The software Trimmomatic v.0.39 was used to trim reads, removing adapters and low quality bases (71). STAR v.2.5.4b was used to align reads to the *C. glabrata* CBS 138 reference genome, version s02-m07-r23 (72). One mismatch was allowed per read. HTSeq v.0.6.1 was used to generate the gene count matrix on "intersection-nonempty" mode (73). R version 3.5.1 and Bioconductor release 3.6 were used to perform all statistical analyses on the RNA-seq data. The intersection of genes identified as statistically significantly differentially expressed with a Benjamini-Hochberg corrected false discovery rate of less than 5% by DESeq2 v.1.18.0 was used in downstream analyses (74, 75).

Quantitative real-time PCR analysis

RNA was isolated from cells by standard acid phenol purification. Reverse transcription was performed using the ABM all-in-one 5X RT Mastermix kit (ABM, Richmond, Canada). Primer Express 3.0 software was used for designing primers and quantitative

real-time polymerase chain reaction (qRT-PCR) was performed as previously described (28, 76, 77). A minimum of three biological replicates, including three technical replicates, were performed for all samples. Data were analyzed using the ΔΔCt method where *RDN18* (18S ribosomal RNA) was used as an internal control. All samples were normalized to an untreated, untagged WT strain.

Minimal inhibitory concentration assay

MIC assays were performed based on a modified version of the CLSI method for testing yeast, 3rd addition (78). Briefly, yeast strains were inoculated in SC media and grown to saturation overnight. The indicated strains were diluted to an OD_{600} of 0.003 in in SC or RPMI media. Cells were mixed with fluconazole (Cayman Chemical) for a final volume of 100µl per well in a 96 well polystyrene microplate with concentrations of fluconazole ranging from 0-256 µg/mL. Plates were incubated at 35˚C and MICs were recorded at 24 hours. MICs were determined visually and were counted as wells where >90% of growth was inhibited.

Nile Red Assay

Fluorescence-based Nile red assays were performed as previously described (46). Briefly, cells were grown overnight in SC media to saturation. Cells were back diluted to an $O.D._{600}$ of 0.1 and grown for 6 hours. Cells were collected then washed with PBS twice and incubated in 1.5mL of PBS+2% glucose for 1 hour. Next, 2.87 µL of a 1mg/mL stock of Nile red (Sigma) was added to each sample and incubated at 30°C shaking for an additional 30 minutes. Samples were washed twice with PBS and placed in triplicate in a black 96-well flat-bottomed polystyrene microplate. Fluorescence was

detected using a Bio-Tek Synergy 4 multimode plate reader using an excitation wavelength of 553nm and an emission wavelength of 636nm.

Chromatin Immunoprecipitation

ZipChIP was performed as previously described (69). Briefly, 50 ml cultures were grown to log phase (OD_{600} of 0.6) in SC complete media at 30° shaking. Treated cells were dosed with 64µg/mL fluconazole (Cayman Chemical) at an OD_{600} of 0.2 for 3 hours. Additionally, cultures were grown to saturation, back diluted to an $O.D._{600}$ of 0.6, treated with 64µg/mL fluconazole for 3 hours and collected. Cells were formaldehyde cross-linked and harvested as previously described (69). Cell lysates were precleared with 5 µl of unbound Protein G magnetic beads for 30 min rotating at 4°. A total of 12.5 µl of precleared lysate was immunoprecipitated with 10 µl of Protein G magnetic beads (10004D; Life Technologies) conjugated to 1 µl of Histone H3K4me3 antibody (Millipore 07-473) or Histone H3 antibody (Abcam ab1791). Probe sets used in qRT-PCR are described in supplemental Table S5.

ACKNOWLEGEMENTS

This work was supported by grants from the National Institutes of Health to S.D.B (AI136995), the Purdue Department of Biochemistry Bird Stair Fellowship (to K.M.B.), Purdue Center for Cancer Research (Grant P30CA023168: DNA Sequencing Shared Resource and Collaborative Core for Cancer Bioinformatics at Purdue), Walther Cancer Foundation and the IU Simon Cancer Center (Grant P30CA082709). Additional funding

542 support was provided by the NIFA 1007570 (S.D.B). We thank the Purdue

543 Bioinformatics Core for their pipelines and bioinformatics software.

544

545

REFERENCES

1. Wisplinghoff H, Bischoff T, Tallent SM, Seifert H, Wenzel RP, Edmond MB. 2004. Nosocomial bloodstream infections in US hospitals: Analysis of 24,179 cases from a prospective nationwide surveillance study. Clinical Infectious Diseases 39:309-317.
2. Wisplinghoff H, Ebbers J, Geurtz L, Stefanik D, Major Y, Edmond MB, Wenzel RP, Seifert H. 2014. Nosocomial bloodstream infections due to Candida spp. in the USA: species distribution, clinical features and antifungal susceptibilities. International Journal of Antimicrobial Agents 43:78-81.
3. Chen S, Slavin M, Nguyen Q, Marriott D, Playford EG, Ellis D, Sorrell T, Study AC. 2006. Active surveillance for candidemia, Australia. Emerg Infect Dis 12:1508-16.
4. Chouhan S, Kallianpur S, Prabhu KT, Tijare M, Kasetty S, Gupta S. 2019. Candidal Prevalence in Diabetics and its Species Identification. Int J Appl Basic Med Res 9:49-54.
5. Khatib R, Johnson LB, Fakih MG, Riederer K, Briski L. 2016. Current trends in candidemia and species distribution among adults: Candida glabrata surpasses C. albicans in diabetic patients and abdominal sources. Mycoses 59:781-786.
6. Hachem R, Hanna H, Kontoyiannis D, Jiang Y, Raad I. 2008. The changing epidemiology of invasive candidiasis: Candida glabrata and Candida krusei as the leading causes of candidemia in hematologic malignancy. Cancer 112:2493-9.
7. Vermitsky JP, Edlind TD. 2004. Azole resistance in Candida glabrata: coordinate upregulation of multidrug transporters and evidence for a Pdr1-like transcription factor. Antimicrob Agents Chemother 48:3773-81.
8. Pelz RK, Lipsett PA, Swoboda SM, Diener-West M, Powe NR, Brower RG, Perl TM, Hammond JM, Hendrix CW. 2000. Candida infections: Outcome and attributable ICU costs in critically ill patients. Journal of Intensive Care Medicine 15:255-261.
9. Rentz AM, Halpern MT, Bowden R. 1998. The impact of candidemia on length of hospital stay, outcome, and overall cost of illness. Clinical Infectious Diseases 27:781-788.
10. Pfaller MA, Jones RN, Messer SA, Edmond MB, Wenzel RP, Grp SP. 1998. National surveillance of nosocomial blood stream infection due to species of Candida other than Candida albicans: Frequency of occurrence and antifungal susceptibility in the SCOPE program. Diagnostic Microbiology and Infectious Disease 30:121-129.
11. Pappas PG, Kauffman CA, Andes DR, Clancy CJ, Marr KA, Ostrosky-Zeichner L, Reboli AC, Schuster MG, Vazquez JA, Walsh TJ, Zaoutis TE, Sobel JD. 2016. Clinical Practice Guideline for the Management of Candidiasis: 2016 Update by the Infectious Diseases Society of America. Clin Infect Dis 62:e1-50.
12. Whaley SG, Rogers PD. 2016. Azole Resistance in Candida glabrata. Curr Infect Dis Rep 18:41.
13. Tscherner M, Schwarzmüller T, Kuchler K. 2011. Pathogenesis and Antifungal Drug Resistance of the Human Fungal Pathogen Candida glabrata. Pharmaceuticals (Basel) 4:169-86.
14. Tsai HF, Krol AA, Sarti KE, Bennett JE. 2006. Candida glabrata PDR1, a transcriptional regulator of a pleiotropic drug resistance network, mediates azole resistance in clinical isolates and petite mutants. Antimicrob Agents Chemother 50:1384-92.
15. Galkina KV, Okamoto M, Chibana H, Knorre DA, Kajiwara S. 2020. Deletion of CDR1 reveals redox regulation of pleiotropic drug resistance in Candida glabrata. Biochimie 170:49-56.
16. Warrilow AG, Mullins JG, Hull CM, Parker JE, Lamb DC, Kelly DE, Kelly SL. 2012. S279 point mutations in Candida albicans Sterol 14-α demethylase (CYP51) reduce in vitro inhibition by fluconazole. Antimicrob Agents Chemother 56:2099-107.

17. Flowers SA, Barker KS, Berkow EL, Toner G, Chadwick SG, Gygax SE, Morschhäuser J, Rogers PD. 2012. Gain-of-function mutations in UPC2 are a frequent cause of ERG11 upregulation in azole-resistant clinical isolates of Candida albicans. Eukaryot Cell 11:1289-99.
18. Sanguinetti M, Posteraro B, Fiori B, Ranno S, Torelli R, Fadda G. 2005. Mechanisms of azole resistance in clinical isolates of Candida glabrata collected during a hospital survey of antifungal resistance. Antimicrob Agents Chemother 49:668-79.
19. Whaley SG, Berkow EL, Rybak JM, Nishimoto AT, Barker KS, Rogers PD. 2017. Azole Antifungal Resistance in Candida albicans and Emerging Non-albicans Candida Species. Frontiers in Microbiology 7:2173.
20. Sanglard D, Ischer F, Calabrese D, Majcherczyk PA, Bille J. 1999. The ATP binding cassette transporter gene CgCDR1 from Candida glabrata is involved in the resistance of clinical isolates to azole antifungal agents. Antimicrob Agents Chemother 43:2753-65.
21. O'Kane CJ, Hyland EM. 2019. Yeast epigenetics: the inheritance of histone modification states. Biosci Rep 39:1-13.
22. Li X, Cai Q, Mei H, Zhou X, Shen Y, Li D, Liu W. 2015. The Rpd3/Hda1 family of histone deacetylases regulates azole resistance in Candida albicans. J Antimicrob Chemother 70:1993-2003.
23. Robbins N, Leach MD, Cowen LE. 2012. Lysine deacetylases Hda1 and Rpd3 regulate Hsp90 function thereby governing fungal drug resistance. Cell Rep 2:878-88.
24. Shivarathri R, Tscherner M, Zwolanek F, Singh NK, Chauhan N, Kuchler K. 2019. The Fungal Histone Acetyl Transferase Gcn5 Controls Virulence of the Human Pathogen Candida albicans through Multiple Pathways. Sci Rep 9:9445.
25. Lopes da Rosa J, Boyartchuk VL, Zhu LJ, Kaufman PD. 2010. Histone acetyltransferase Rtt109 is required for Candida albicans pathogenesis. Proc Natl Acad Sci U S A 107:1594-9.
26. Orta-Zavalza E, Guerrero-Serrano G, Gutierrez-Escobedo G, Canas-Villamar I, Juarez-Cepeda J, Castano I, De Las Penas A. 2013. Local silencing controls the oxidative stress response and the multidrug resistance in Candida glabrata. Mol Microbiol 88:1135-48.
27. Filler EE, Liu Y, Solis NV, Wang L, Diaz LF, Edwards JE, Filler SG, Yeaman MR. 2021. Identification of Candida glabrata Transcriptional Regulators That Govern Stress Resistance and Virulence. Infect Immun 89:3.
28. South PF, Harmeyer KM, Serratore ND, Briggs SD. 2013. H3K4 methyltransferase Set1 is involved in maintenance of ergosterol homeostasis and resistance to Brefeldin A. 10:E1016-E1025.
29. Serratore ND, Baker KM, Macadlo LA, Gress AR, Powers BL, Atallah N, Westerhouse KM, Hall MC, Weake VM, Briggs SD. 2018. A Novel Sterol-Signaling Pathway Governs Azole Antifungal Drug Resistance and Hypoxic Gene Repression in. Genetics 208:1037-1055.
30. Raman S, Nguyen M, Zhang Z, Cheng S, Jia H, Weisner N, Iczkowski K, Clancy C. 2006. Candida albicans SET1 encodes a histone 3 lysine 4 methyltransferase that contributes to the pathogenesis of invasive candidiasis. Mol Microbiol 60:697-709.
31. Briggs SD, Bryk M, Strahl BD, Cheung WL, Davie JK, Dent SY, Winston F, Allis CD. 2001. Histone H3 lysine 4 methylation is mediated by Set1 and required for cell growth and rDNA silencing in Saccharomyces cerevisiae. Genes Dev 15:3286-95.
32. Roguev A, Schaft D, Shevchenko A, Pijnappel WW, Wilm M, Aasland R, Stewart AF. 2001. The Saccharomyces cerevisiae Set1 complex includes an Ash2 homologue and methylates histone 3 lysine 4. EMBO J 20:7137-48.

644 33. Nagy PL, Griesenbeck J, Kornberg RD, Cleary ML. 2002. A trithorax-group complex
645 purified from Saccharomyces cerevisiae is required for methylation of histone H3. Proc
646 Natl Acad Sci U S A 99:90-4.
647 34. Dehe PM, Dichtl B, Schaft D, Roguev A, Pamblanco M, Lebrun R, Rodriguez-Gil A,
648 Mkandawire M, Landsberg K, Shevchenko A, Shevchenko A, Rosaleny LE, Tordera V,
649 Chavez S, Stewart AF, Geli V. 2006. Protein interactions within the Set1 complex and
650 their roles in the regulation of histone 3 lysine 4 methylation. J Biol Chem 281:35404-12.
651 35. Takahashi YH, Westfield GH, Oleskie AN, Trievel RC, Shilatifard A, Skiniotis G. 2011.
652 Structural analysis of the core COMPASS family of histone H3K4 methylases from yeast
653 to human. Proc Natl Acad Sci U S A 108:20526-31.
654 36. Mersman DP, Du HN, Fingerman IM, South PF, Briggs SD. 2012. Charge-based
655 interaction conserved within histone H3 lysine 4 (H3K4) methyltransferase complexes is
656 needed for protein stability, histone methylation, and gene expression. J Biol Chem
657 287:2652-65.
658 37. Shilatifard A. 2012. The COMPASS family of histone H3K4 methylases: mechanisms of
659 regulation in development and disease pathogenesis. Annu Rev Biochem 81:65-95.
660 38. Mueller JE, Canze M, Bryk M. 2006. The requirements for COMPASS and Paf1 in
661 transcriptional silencing and methylation of histone H3 in Saccharomyces cerevisiae.
662 Genetics 173:557-67.
663 39. Eissenberg JC, Shilatifard A. 2010. Histone H3 lysine 4 (H3K4) methylation in
664 development and differentiation. Dev Biol 339:240-9.
665 40. Zordan R, Ren Y, Pan S, Rotondo G, De Las Penas A, Lluore J, Cormack B. 2013.
666 Expression plasmids for use in Candida glabrata.
667 doi:*10.1534/g3.113.006908.* 10.1534/g3.113.006908:1675-86.
668 41. Schlichter A, Cairns BR. 2005. Histone trimethylation by Set1 is coordinated by the
669 RRM, autoinhibitory, and catalytic domains. EMBO J 24:1222-31.
670 42. Soares LM, Radman-Livaja M, Lin SG, Rando OJ, Buratowski S. 2014. Feedback
671 control of Set1 protein levels is important for proper H3K4 methylation patterns. Cell Rep
672 6:961-972.
673 43. Kitada K, Yamaguchi E, Arisawa M. 1995. Cloning of the Candida glabrata TRP1 and
674 HIS3 genes, and construction of their disruptant strains by sequential integrative
675 transformation. Gene 165:203-6.
676 44. Vermitsky JP, Earhart KD, Smith WL, Homayouni R, Edlind TD, Rogers PD. 2006. Pdr1
677 regulates multidrug resistance in Candida glabrata: gene disruption and genome-wide
678 expression studies. Mol Microbiol 61:704-22.
679 45. Whaley SG, Zhang Q, Caudle KE, Rogers PD. 2018. Relative Contribution of the ABC
680 Transporters Cdr1, Pdh1, and Snq2 to Azole Resistance in Candida glabrata. Antimicrob
681 Agents Chemother 62:10.
682 46. Tsao S, Weber S, Cameron C, Nehme D, Ahmadzadeh E, Raymond M. 2016. Positive
683 regulation of the Candida albicans multidrug efflux pump Cdr1p function by
684 phosphorylation of its N-terminal extension. Journal of Antimicrobial Chemotherapy
685 71:3125-3134.
686 47. Ivnitski-Steele I, Holmes A, Lamping E, Monk B, Cannon R, Sklar L. 2009. Identification
687 of Nile red as a fluorescent substrate of the Candida albicans ATP-binding cassette
688 transporters Cdr1p and Cdr2p and the major facilitator superfamily transporter Mdr1p.
689 Analytical biochemistry 394:87-91.
690 48. Flowers SA, Colon B, Whaley SG, Schuler MA, Rogers PD. 2015. Contribution of
691 clinically derived mutations in ERG11 to azole resistance in Candida albicans.
692 Antimicrob Agents Chemother 59:450-60.
693 49. Kelly SL, Lamb DC, Kelly DE. 1997. Sterol 22-desaturase, cytochrome P45061,
694 possesses activity in xenobiotic metabolism. FEBS Lett 412:233-5.

50. Morio F, Pagniez F, Lacroix C, Miegeville M, Le Pape P. 2012. Amino acid substitutions in the Candida albicans sterol Delta5,6-desaturase (Erg3p) confer azole resistance: characterization of two novel mutants with impaired virulence. J Antimicrob Chemother 67:2131-8.
51. Kelly SL, Lamb DC, Kelly DE, Manning NJ, Loeffler J, Hebart H, Schumacher U, Einsele H. 1997. Resistance to fluconazole and cross-resistance to amphotericin B in Candida albicans from AIDS patients caused by defective sterol delta5,6-desaturation. FEBS Lett 400:80-2.
52. Watson PF, Rose ME, Ellis SW, England H, Kelly SL. 1989. Defective sterol C5-6 desaturation and azole resistance: a new hypothesis for the mode of action of azole antifungals. Biochem Biophys Res Commun 164:1170-5.
53. Vu B, Thomas G, Moye-Rowley W. 2019. Evidence that Ergosterol Biosynthesis Modulates Activity of the Pdr1 Transcription Factor in Candida glabrata. mBio 10.
54. Moye-Rowley WS. 2020. Linkage between genes involved in azole resistance and ergosterol biosynthesis. PLoS Pathog 16:e1008819.
55. Yu SJ, Chang YL, Chen YL. 2018. Deletion of ADA2 Increases Antifungal Drug Susceptibility and Virulence in Candida glabrata. Antimicrob Agents Chemother 62:3.
56. Zavrel M, Hoot SJ, White TC. 2013. Comparison of sterol import under aerobic and anaerobic conditions in three fungal species, Candida albicans, Candida glabrata, and Saccharomyces cerevisiae. Eukaryot Cell 12:725-38.
57. Zhang L, Xu W. 2015. Histone deacetylase inhibitors for enhancing activity of antifungal agent: a patent evaluation of WO2014041424(A1). Expert Opin Ther Pat 25:237-40.
58. Mai A, Rotili D, Massa S, Brosch G, Simonetti G, Passariello C, Palamara AT. 2007. Discovery of uracil-based histone deacetylase inhibitors able to reduce acquired antifungal resistance and trailing growth in Candida albicans. Bioorg Med Chem Lett 17:1221-5.
59. Hnisz D, Majer O, Frohner IE, Komnenovic V, Kuchler K. 2010. The Set3/Hos2 histone deacetylase complex attenuates cAMP/PKA signaling to regulate morphogenesis and virulence of Candida albicans. PLoS Pathog 6:e1000889.
60. Pfaller MA, Messer SA, Georgopapadakou N, Martell LA, Besterman JM, Diekema DJ. 2009. Activity of MGCD290, a Hos2 histone deacetylase inhibitor, in combination with azole antifungals against opportunistic fungal pathogens. J Clin Microbiol 47:3797-804.
61. Pfaller MA, Rhomberg PR, Messer SA, Castanheira M. 2015. In vitro activity of a Hos2 deacetylase inhibitor, MGCD290, in combination with echinocandins against echinocandin-resistant Candida species. Diagn Microbiol Infect Dis 81:259-63.
62. Smith WL, Edlind TD. 2002. Histone deacetylase inhibitors enhance Candida albicans sensitivity to azoles and related antifungals: correlation with reduction in CDR and ERG upregulation. Antimicrob Agents Chemother 46:3532-9.
63. Kim T, Buratowski S. 2009. Dimethylation of H3K4 by Set1 recruits the Set3 histone deacetylase complex to 5' transcribed regions. Cell 137:259-72.
64. Pijnappel WW, Schaft D, Roguev A, Shevchenko A, Tekotte H, Wilm M, Rigaut G, Seraphin B, Aasland R, Stewart AF. 2001. The S. cerevisiae SET3 complex includes two histone deacetylases, Hos2 and Hst1, and is a meiotic-specific repressor of the sporulation gene program. Genes Dev 15:2991-3004.
65. Zhou Y, Liao M, Zhu C, Hu Y, Tong T, Peng X, Li M, Feng M, Cheng L, Ren B, Zhou X. 2018. ERG3 and ERG11 genes are critical for the pathogenesis of Candida albicans during the oral mucosal infection. Int J Oral Sci 10:9.
66. Becker JM, Kauffman SJ, Hauser M, Huang L, Lin M, Sillaots S, Jiang B, Xu D, Roemer T. 2010. Pathway analysis of Candida albicans survival and virulence determinants in a murine infection model. Proc Natl Acad Sci U S A 107:22044-9.

67. Miyazaki T, Miyazaki Y, Izumikawa K, Kakeya H, Miyakoshi S, Bennett JE, Kohno S. 2006. Fluconazole treatment is effective against a Candida albicans erg3/erg3 mutant in vivo despite in vitro resistance. Antimicrob Agents Chemother 50:580-6.
68. Fingerman IM, Wu CL, Wilson BD, Briggs SD. 2005. Global loss of Set1-mediated H3 Lys4 trimethylation is associated with silencing defects in Saccharomyces cerevisiae. J Biol Chem 280:28761-5.
69. Harmeyer KM, South PF, Bishop B, Ogas J, Briggs SD. 2015. Immediate chromatin immunoprecipitation and on-bead quantitative PCR analysis: a versatile and rapid ChIP procedure. Nucleic Acids Res 43:e38.
70. Agarwal AK, Rogers PD, Baerson SR, Jacob MR, Barker KS, Cleary JD, Walker LA, Nagle DG, Clark AM. 2003. Genome-wide expression profiling of the response to polyene, pyrimidine, azole, and echinocandin antifungal agents in Saccharomyces cerevisiae. J Biol Chem 278:34998-5015.
71. Dobin A, Davis CA, Schlesinger F, Drenkow J, Zaleski C, Jha S, Batut P, Chaisson M, Gingeras TR. 2013. STAR: ultrafast universal RNA-seq aligner. Bioinformatics 29:15-21.
72. Anders S, Pyl PT, Huber W. 2015. HTSeq-a Python framework to work with high-throughput sequencing data. Bioinformatics 31:166-169.
73. Zanini F, Anders S. 2021(in preparation). HTSeq 2.0 – Efficient manipulation of high-throughput sequencing data with long genomes.
74. Benjamini Y, Hochberg Y. 1995. Controlling the False Discovery Rate - a Practical and Powerful Approach to Multiple Testing. Journal of the Royal Statistical Society Series B-Statistical Methodology 57:289-300.
75. Love MI, Huber W, Anders S. 2014. Moderated estimation of fold change and dispersion for RNA-seq data with DESeq2. Genome Biology 15:550.
76. Zhang Y, Serratore ND, Briggs SD. 2017. N-ICE plasmids for generating N-terminal 3 x FLAG tagged genes that allow inducible, constitutive or endogenous expression in Saccharomyces cerevisiae. Yeast 34:223-235.
77. South PF, Fingerman IM, Mersman DP, Du HN, Briggs SD. 2010. A conserved interaction between the SDI domain of Bre2 and the Dpy-30 domain of Sdc1 is required for histone methylation and gene expression. J Biol Chem 285:595-607.
78. CLSI. Reference Method for Broth Dilution Antifungal Susceptibility Testing of Yeasts; Approved Standard—Third Edition. 2008. CLSI document M27-A3, Wayne, PA: Clinical and Laboratory Standards Institute.

FIGURE LEGENDS

FIG 1 *Loss of Set1-mediated mono-, di-, and trimethylation at histone H3K4 in Saccharomyces cerevisiae and Candida glabrata results in increased azole susceptibility and delayed growth in vitro.* (A) Five-fold serial dilution spot assays of the indicated *S. cerevisiae* strains were grown on SC media with and without 8 µg/mL fluconazole and incubated at 30ºC for 72 hours. (B & D) Whole cell extracts isolated from the indicated strains were immunoblotted using histone H3K4 methyl-specific mono-, di- and trimethylation antibodies of whole cell extracts isolated from the indicated strains. Histone H3 was used as a loading control. (C) Five-fold serial dilution spot assays of the indicated *C. glabrata* strains were grown on SC media with and without 32 µg/mL fluconazole and incubated at 30ºC for 48 hours. (E) Liquid growth curve assay of the indicated *C. glabrata* strains grown over 50 hours with or without 32 µg/mL fluconazole.

FIG 2 *Deletion of Set1 complex members in C. glabrata results in increased azole susceptibility and loss of histone H3K4 methylation*. (A) MIC assay of the indicated strains performed in RPMI 1640 media at 35°C and results recorded after 48 hours of incubation. (B) Five-fold serial dilution spot assays of the indicated *C. glabrata* strains were grown on SC plates with or without 32 µg/ml fluconazole. (C) Whole cell extracts isolated from the indicated strains were immunoblotted using H3K4 methyl-specific mono-, di- and trimethylation antibodies. Histone H3 was used as a loading control.

FIG 3 *The catalytic activity of the SET domain is necessary for Set1-mediated histone H3K4 methylation and increased azole susceptibility in C. glabrata.* (A)

Five-fold serial dilution spot assays of the indicated C. glabrata strains were grown on SC plates with or without 32 µg/ml fluconazole. (B) Whole cell extracts isolated from the indicated strains were immunoblotted using methyl-specific mono-, di- and trimethylation antibodies. Histone H3 was used as a loading control.

FIG 4 *Deletion of SET1 in C. glabrata does not alter gene expression levels or function of the efflux drug transporter, CDR1 or transcription factor PDR1.* (A and B) Expression of indicated genes was determined in *Cg*WT and *Cgset1Δ* strain cells treated with and without 64 µg/ml fluconazole for 3 hr by qRT-PCR analysis. Gene expression analysis was set relative to the untreated wild-type and expression was normalized to *RDN18* mRNA levels. Data were analyzed from ≥ 3 biological replicates with three technical replicates each. Error bars represent SD. (C) Red fluorescence units were measured as output in a Nile Red assay to determine the efficacy of Cdr1 in the indicated strains with and without fluconazole. A *pdr1Δ* strain was used as a control. Data were analyzed from ≥ 3 biological replicates with three technical replicates each. Statistics were performed using Graphpad Prism student t-test version 9.2.0. *ns represents p< 0.05, **p<0.01,* Error bars represent SD.

FIG 5 *The deletion of SET1 in C. glabrata alters global and local levels of gene expression under untreated and azole conditions.* The genome-wide changes in gene expression under azoles were performed using *C. glabrata* CBS138 WT and *set1Δ* strains. (A) The PCA for WT and *set1Δ* azole treated samples relative to WT untreated samples based on the counts per million. (B) Volcano plot showing the significance [$-\log_2$ (FDR), *y*-axis] *vs.* the fold change (*x*-axis) of the DEGs identified in the WT untreated samples relative to *set1Δ* untreated samples. (C) Volcano plot showing the

significance [$-\log_2$ (FDR), *y*-axis] *vs.* the fold change (*x*-axis) of the DEGs identified in the *set1*Δ azole treated samples relative to WT azole treated samples. Genes with significant differential expression (FDR < 0.05) in (B and C) are highlighted in red or blue for up- and downregulated genes, respectively. Black highlighted genes are considered nonsignificant. (D) Genes from the RNA-seq dataset that were statistically significantly enriched (FDR < 0.05) were used for GO term determination of Set1-dependent DEGs under azole conditions. Downregulated genes refer to the DEGs that are dependent on Set1 for activation either directly or indirectly. Significantly enriched groups of GO terms were identified as the DEGs from only *set1*Δ and WT azole treated samples. (E and F) Expression of indicated genes was determined in WT and ***set1Δ*** strain cells treated with 64 µg/ml fluconazole for 3 hr by qRT-PCR analysis. Gene expression analysis was set relative to the untreated wild-type and expression was normalized to *RDN18* mRNA levels. Data were analyzed from ≥ 3 biological replicates with three technical replicates each. Statistics were performed using Graphpad Prism student t-test version 9.2.0.*****p<0.0001 and **p=0.002.* Error bars represent SD..

FIG 6 *Histone H3K4 trimethylation is enriched on ERG gene chromatin and Set1-mediated histone H3K4 methyltransferase activity is required for azole induction of ERG genes.* (A and B) ChIP analysis of histone H3K4 tri-methylation levels at the promoter, 5', and 3' regions of *ERG11* and *ERG3* in a wild-type *C. glabrata* strain with and without 64 µg/mL fluconazole treatment. ChIP analysis was set relative to a ***set1Δ*** strain and normalized to histone H3 and DNA input levels. Data were analyzed from 5 biological replicates with three technical replicates each, **p<0.05.* (C and D) Expression of indicated genes was determined in the indicated mutants treated with and without 64

853 µg/ml fluconazole for 3 hr by qRT-PCR analysis. Gene expression analysis was set
854 relative to the untreated wild-type containing an empty vector and expression was
855 normalized to *RDN18* mRNA levels. Data were analyzed from ≥ 3 biological replicates
856 with three technical replicates each. Statistics were performed using Graphpad Prism
857 student t-test version 9.2.0. ****$p<0.0001$ and **$p<0.01$. Error bars represent SD.

858 **FIG 7** *Model for the role of Set1-H3K4 methylation in epigenetic control of ERG genes*
859 (Biorender). (A) Under aerobic conditions, the Set1 complex mediates histone H3K4
860 methylation on chromatin at *ERG* genes. In the presence of azoles, azole-induced
861 transcriptional activation recruits TFs, RNA Polymerase II, and the Set1 complex to
862 increases Histone H3K4 methylation. This increase in methylation could permit
863 additional recruitment of other co-factors/epigenetic regulator (e.g., Set3 and/or SAGA
864 complex) that contain “reader” domains that recognize and bind to the H3K4 methyl
865 mark. Thus, this Set1-Erg pathway contributes to the intrinsic azole resistance in *C.*
866 *glabrata.* In the absence of Set1, histone H3K4 methylation is abolished and failure of
867 recruiting additional H3K4 methyl “readers” prevent the induction of *ERG* genes, thus
868 making the *C. glabrata* more susceptible to azole treatment.

FIGURES

Figure 1

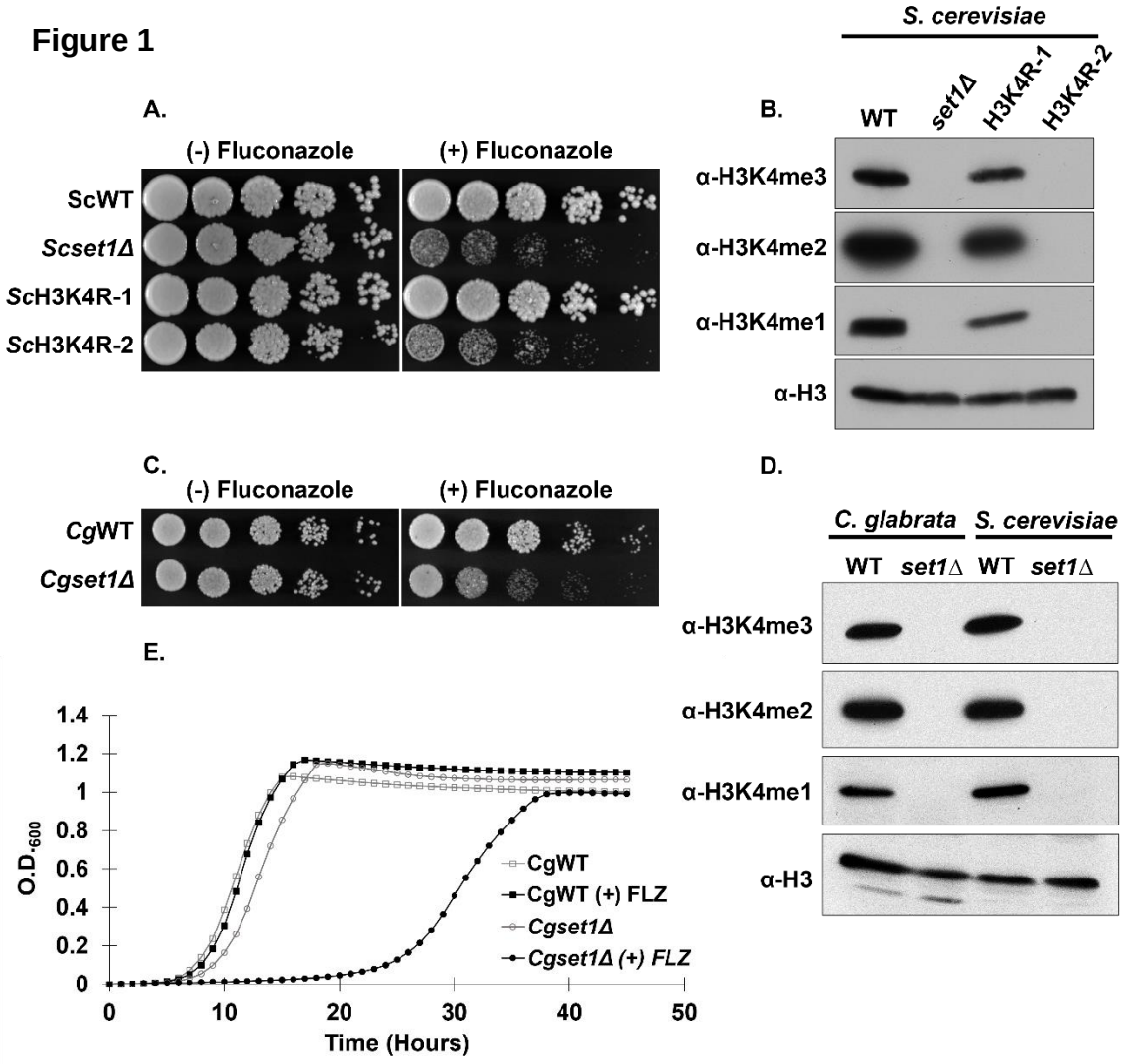

FIG 1 *Loss of Set1-mediated mono-, di-, and trimethylation at histone H3K4 in Saccharomyces cerevisiae and Candida glabrata results in increased azole susceptibility and delayed growth in vitro.* (A) Five-fold serial dilution spot assays of the indicated *S. cerevisiae* strains were grown on SC media with and without 8 µg/mL fluconazole and incubated at 30ºC for 72 hours. (B & D) Whole cell extracts isolated from the indicated strains were immunoblotted using histone H3K4 methyl-specific mono-, di- and trimethylation antibodies of whole cell extracts isolated from the indicated strains. Histone H3 was used as a loading control. (C) Five-fold serial dilution spot assays of the indicated *C. glabrata* strains were grown on SC media with and without 32 µg/mL fluconazole and incubated at 30ºC for 48 hours. (E) Liquid growth curve assay of the indicated *C. glabrata* strains grown over 50 hours with or without 32 µg/mL fluconazole.

Figure 2

A.

Strain (CBS138)	FLZ (µg/mL) in RPMI
*Cg*WT	64
Cgset1Δ	8
Cgswd1Δ	8
Cgspp1Δ	16
Cgbre2Δ	16

B.

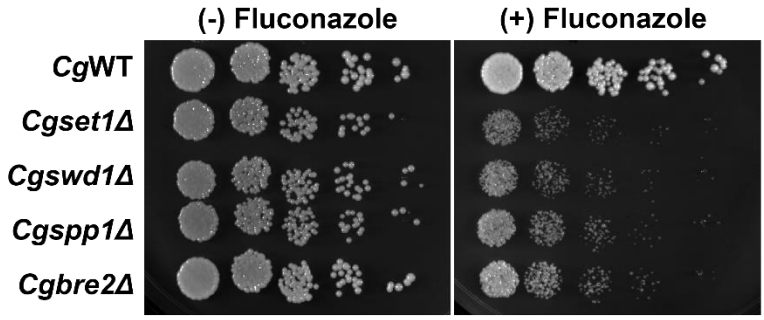

C.

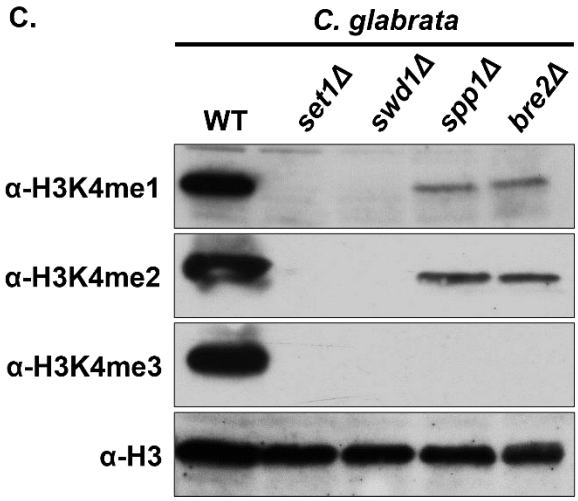

FIG 2 *Deletion of Set1 complex members in C. glabrata results in increased azole susceptibility and loss of histone H3K4 methylation*. (A) MIC assay of the indicated strains performed in RPMI 1640 media at 35°C and results recorded after 48 hours of incubation. (B) Five-fold serial dilution spot assays of the indicated *C. glabrata* strains were grown on SC plates with or without 32 µg/ml fluconazole. (C) Whole cell extracts isolated from the indicated strains were immunoblotted using H3K4 methyl-specific mono-, di- and trimethylation antibodies. Histone H3 was used as a loading control.

Figure 3

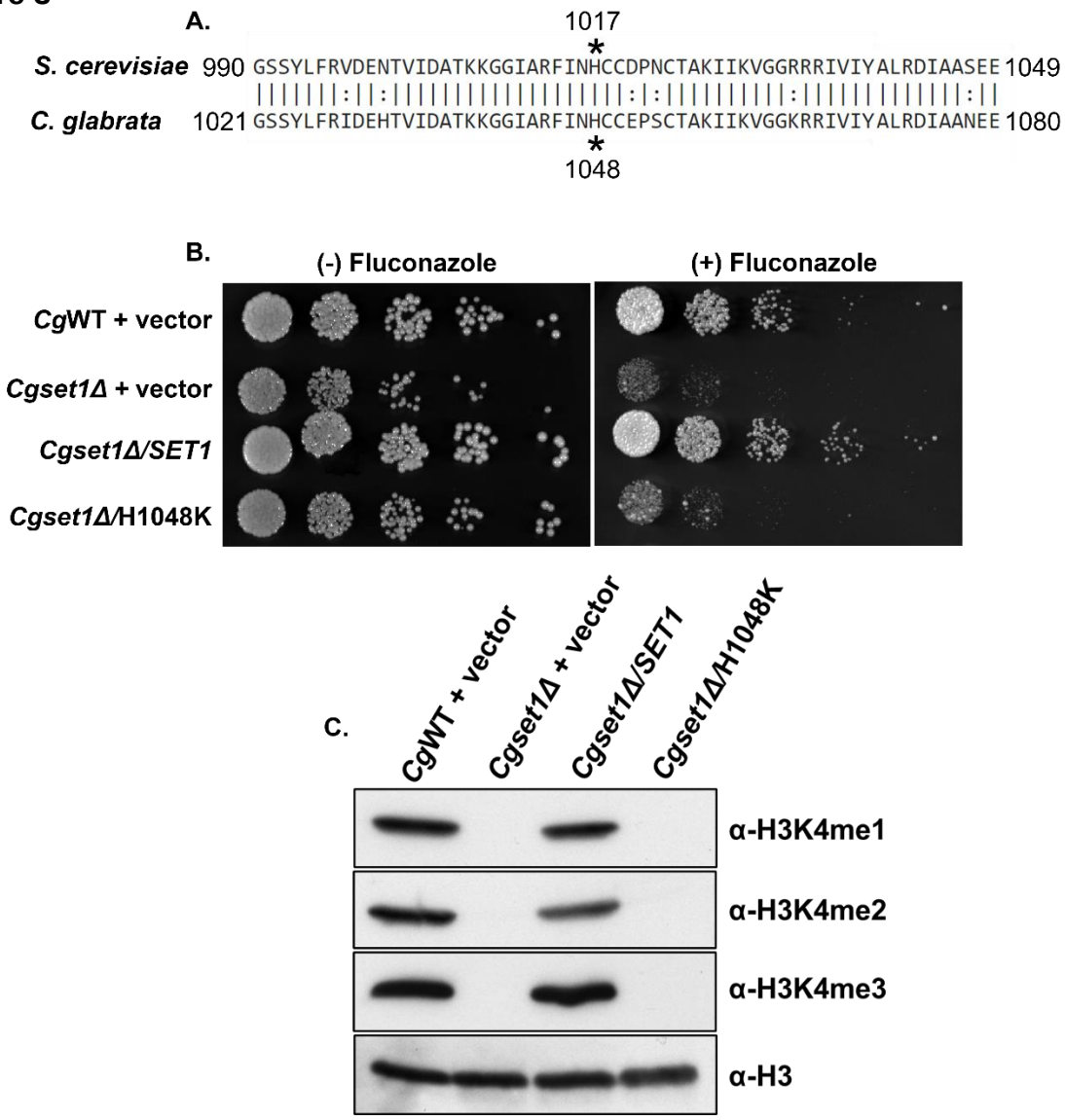

FIG 3 *The catalytic activity of the SET domain is necessary for Set1-mediated histone H3K4 methylation and increased azole susceptibility in C. glabrata* (A) Five-fold serial dilution spot assays of the indicated *C. glabrata* strains were grown on SC plates with or without 32 µg/ml fluconazole. (B) Whole cell extracts isolated from the indicated strains were immunoblotted using methyl-specific mono-, di- and trimethylation antibodies. Histone H3 was used as a loading control

Figure 4

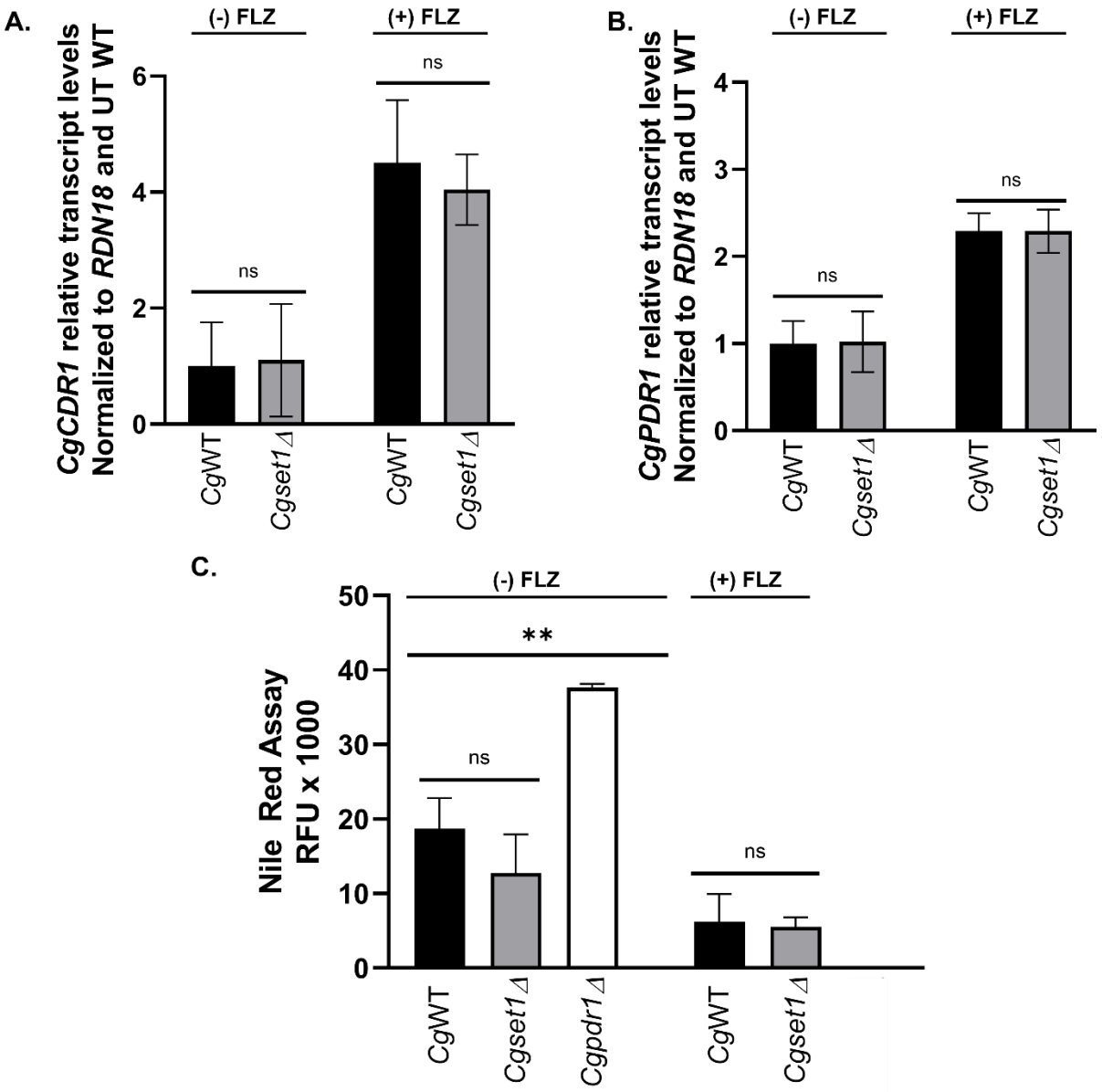

FIG 4 *Deletion of SET1 in C. glabrata does not alter gene expression levels or function of the efflux drug transporter, CDR1 or transcription factor PDR1.* (A and B) Expression of indicated genes was determined in *Cg*WT and *Cgset1Δ* strain cells treated with and without 64 µg/ml fluconazole for 3 hr by qRT-PCR analysis. Gene expression analysis was set relative to the untreated wild-type and expression was normalized to *RDN18* mRNA levels. Data were analyzed from ≥ 3 biological replicates with three technical replicates each. Error bars represent SD. (C) Red fluorescence units were measured as output in a Nile Red assay to determine the efficacy of Cdr1 in the indicated strains with and without fluconazole. A *pdr1Δ* strain was used as a control. Data were analyzed from ≥ 3 biological replicates with three technical replicates each. Statistics were performed using Graphpad Prism student t-test version 9.2.0. *ns represents p< 0.05, **p<0.01,* Error bars represent SD.

Figure 5

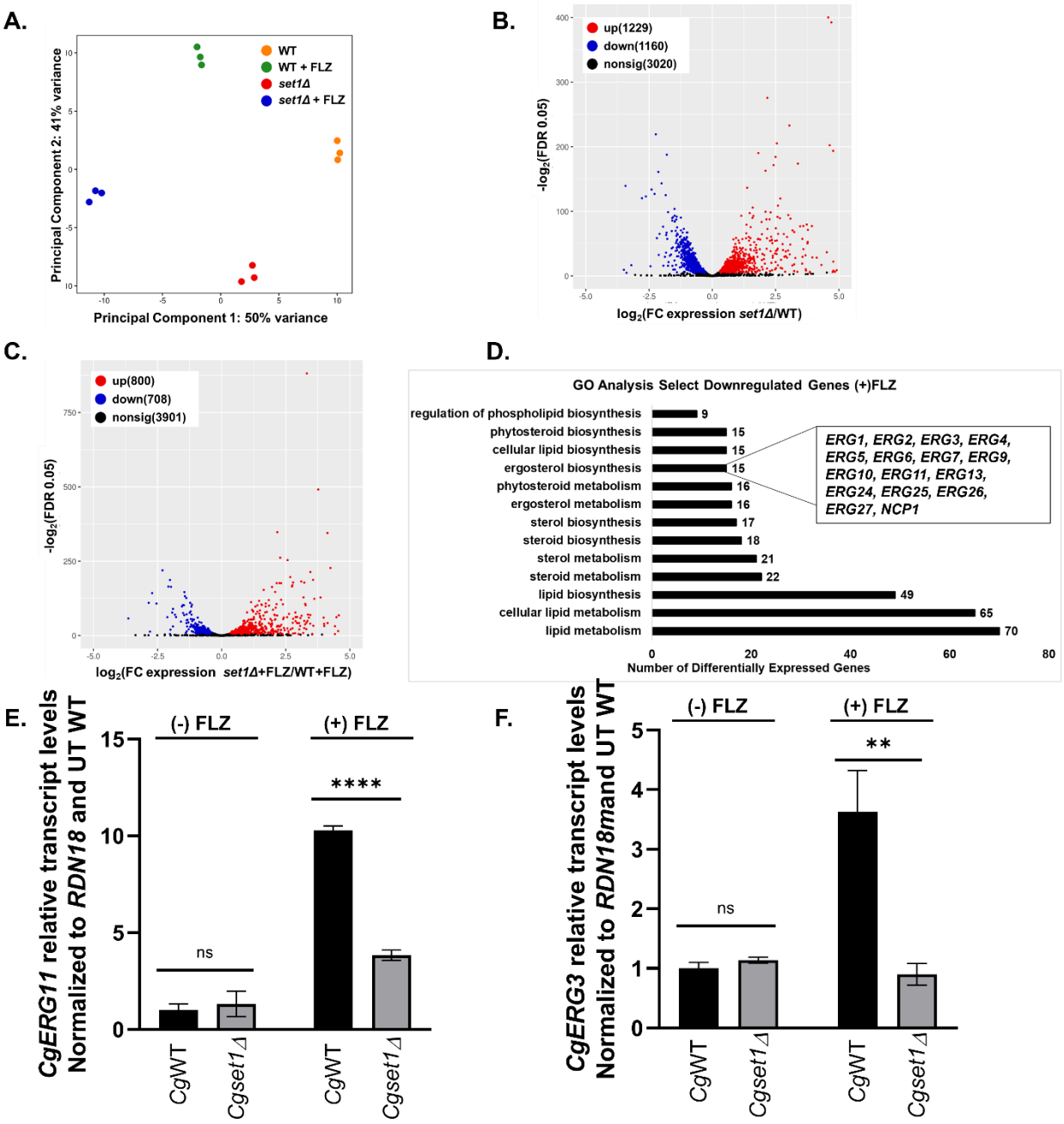

FIG 5 *The deletion of SET1 in C. glabrata alters global and local levels of gene expression under untreated and azole conditions.* The genome-wide changes in gene expression under azoles were performed using *C. glabrata* CBS138 WT and *set1Δ* strains. (A) The PCA for WT and *set1Δ* azole treated samples relative to WT untreated samples based on the counts per million. (B) Volcano plot showing the significance [$-\log_2$ (FDR), *y*-axis] *vs.* the fold change (*x*-axis) of the DEGs identified in the WT untreated samples relative to *set1Δ* untreated samples. (C) Volcano plot showing the significance [$-\log_2$ (FDR), *y*-axis] *vs.* the fold change (*x*-axis) of the DEGs identified in the *set1*Δ azole treated samples relative to WT azole treated samples. Genes with significant differential expression (FDR < 0.05) in (B and C) are highlighted in red or blue for up- and downregulated genes, respectively. Black highlighted genes are

considered nonsignificant. (D) Genes from the RNA-seq dataset that were statistically significantly enriched (FDR < 0.05) were used for GO term determination of Set1-dependent DEGs under azole conditions. Downregulated genes refer to the DEGs that are dependent on Set1 for activation either directly or indirectly. Significantly enriched groups of GO terms were identified as the DEGs from only *set1*Δ and WT azole treated samples. (E and F) Expression of indicated genes was determined in WT and *set1Δ* strain cells treated with 64 µg/ml fluconazole for 3 hr by qRT-PCR analysis. Gene expression analysis was set relative to the untreated wild-type and expression was normalized to *RDN18* mRNA levels. Data were analyzed from ≥ 3 biological replicates with three technical replicates each. Statistics were performed using Graphpad Prism student t-test version 9.2.0.****$p<0.0001$ and **$p=0.002$. Error bars represent SD.

Figure 6

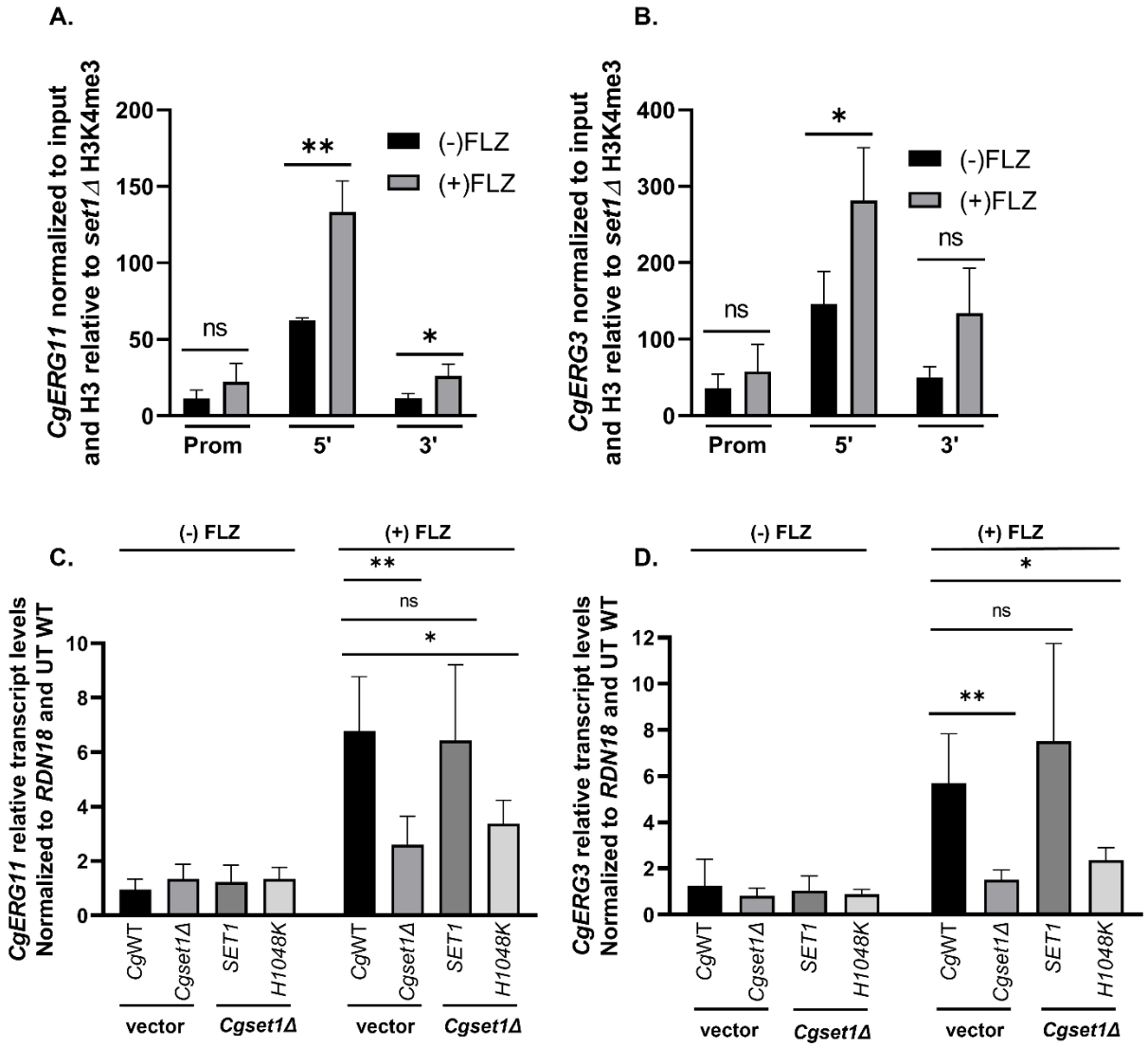

FIG 6 *Histone H3K4 trimethylation is enriched on ERG gene chromatin and Set1-mediated histone H3K4 methyltransferase activity is required for azole induction of ERG genes.* (A and B) ChIP analysis of histone H3K4 tri-methylation levels at the promoter,

5', and 3' regions of *ERG11* and *ERG3* in a wild-type *C. glabrata* strain with and without 64 µg/mL fluconazole treatment. ChIP analysis was set relative to a ***set1Δ*** strain and normalized to histone H3 and DNA input levels. Data were analyzed from 5 biological replicates with three technical replicates each, *$p<0.05$. (C and D) Expression of indicated genes was determined in the indicated mutants treated with and without 64 µg/ml fluconazole for 3 hr by qRT-PCR analysis. Gene expression analysis was set relative to the untreated wild-type containing an empty vector and expression was normalized to *RDN18* mRNA levels. Data were analyzed from ≥ 3 biological replicates with three technical replicates each. Statistics were performed using Graphpad Prism student t-test version 9.2.0. ****$p<0.0001$ and **$p<0.01$. Error bars represent SD.

Figure 7

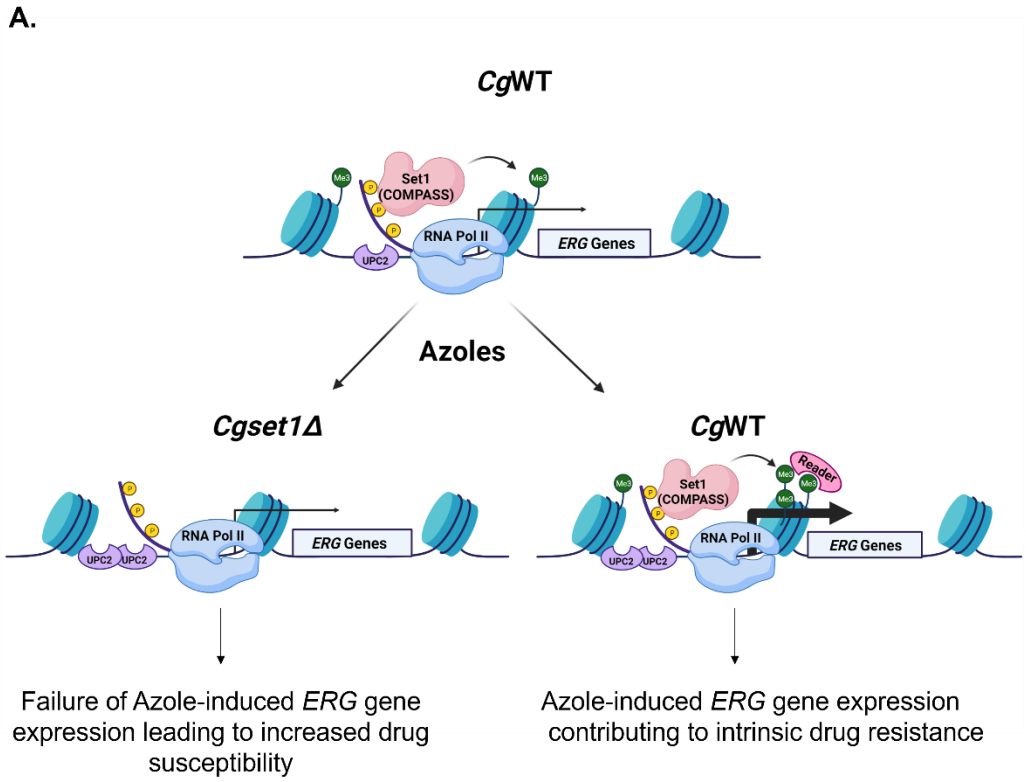

FIG 7 *Model for the role of Set1-H3K4 methylation in epigenetic control of ERG genes* (Biorender). (A) Under aerobic conditions, the Set1 complex mediates histone H3K4 methylation on chromatin at *ERG* genes. In the presence of azoles, azole-induced transcriptional activation recruits TFs, RNA Polymerase II, and the Set1 complex to increases Histone H3K4 methylation. This increase in methylation could permit additional recruitment of other co-factors/epigenetic regulator (e.g., Set3 and/or SAGA complex) that contain "reader" domains that recognize and bind to the H3K4 methyl mark. Thus, this Set1-Erg pathway contributes to the intrinsic azole resistance in *C. glabrata.* In the absence of Set1, histone H3K4 methylation is abolished and failure of recruiting additional H3K4 methyl "readers" prevent the induction of *ERG* genes, thus making the *C. glabrata* more susceptible to azole treatment.

963 **Figure S1**

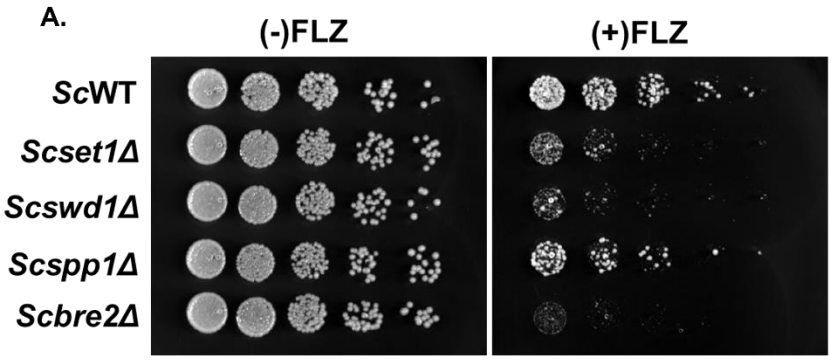

B.

Strain (CBS 138)	FLZ (µg/mL)
WT+vector	128
set1Δ+vector	32
set1Δ+SET1	128
set1Δ+H1048K	32

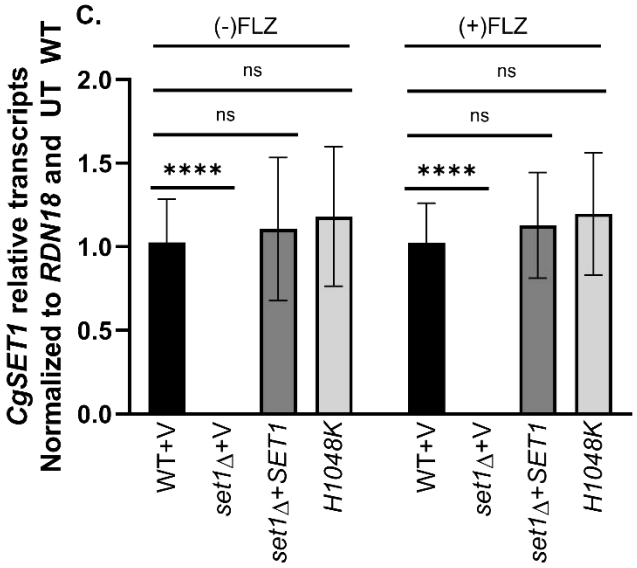

964
965 **FIG S1.** Loss of Set1 complex members results in altered azole efficacy. (A) Five-fold
966 serial dilution spot assays of the indicated S. cerevisiae strains were grown on SC
967 plates with or without 8 µg/ml fluconazole. (B) MIC assay of the indicated strains
968 performed in SC media at 35°C and results recorded after 24 hours of incubation. (C)
969 Expression of SET1 was determined in the indicated mutants treated with and without
970 64 µg/ml fluconazole for 3 hr by qRT-PCR analysis. Gene expression analysis was set
971 relative to the untreated wild-type and expression was normalized to RDN18 mRNA
972 levels. Data were analyzed from 4 biological replicates with three technical replicates
973 each. Statistics were performed using Graphpad Prism student t-test version 9.2.0.
974 ****p<0.0001. Error bars represent SD.
975
976
977

Figure S2

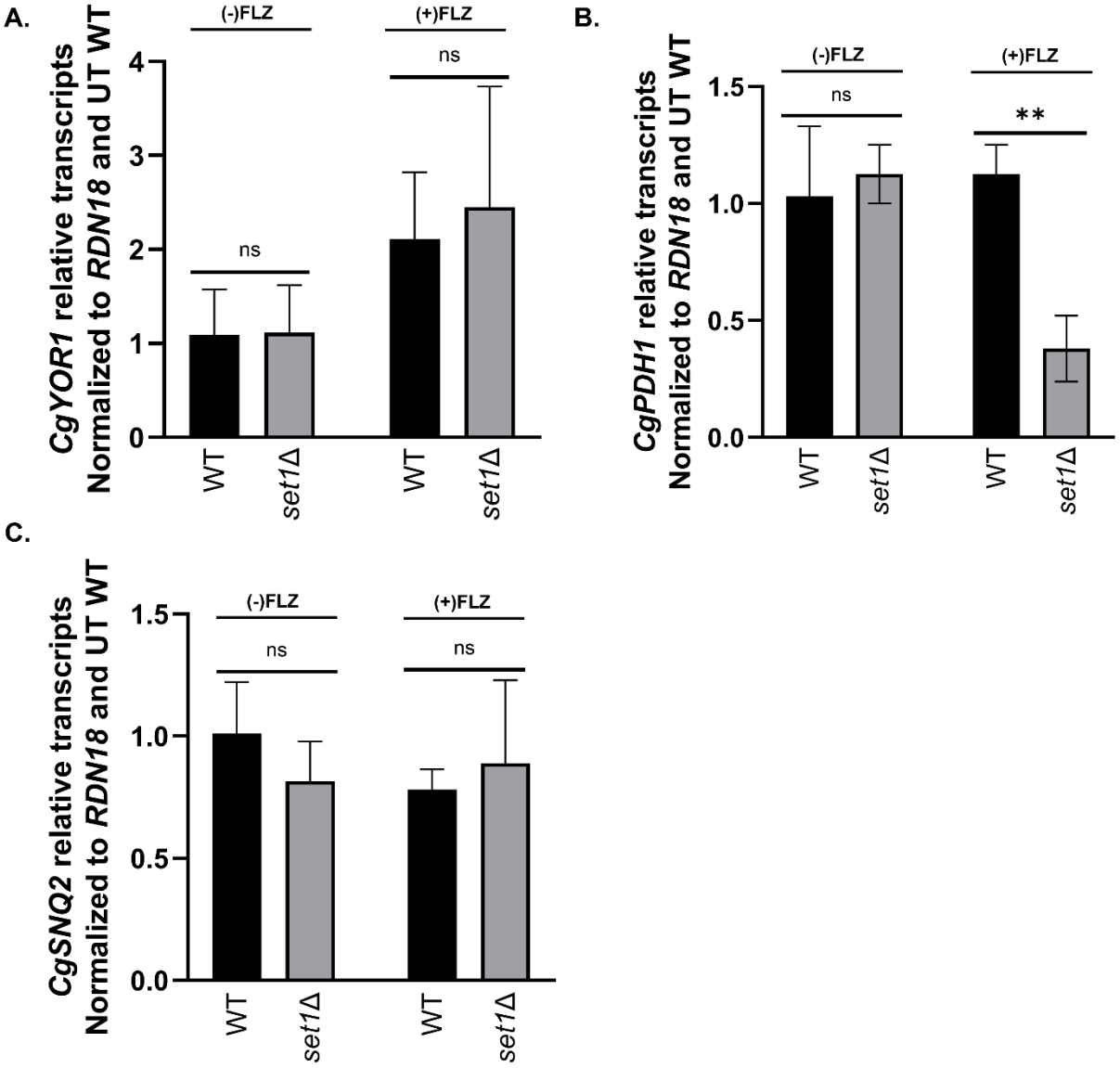

Fig S2. *Transcript levels of drug transporters in a set1Δ strain compared to wild-type.* Expression of the indicated genes were determined in the indicated mutants treated with and without 64 µg/ml fluconazole for 3 hr by qRT-PCR analysis. Gene expression analysis was set relative to the untreated wild-type and expression was normalized to *RDN18* mRNA levels. Data were analyzed from ≥ 3 biological replicates with three technical replicates each. Statistics were performed using Graphpad Prism student t-test version 9.2.0. ***p<0.01.* Error bars represent SD.

Figure S3

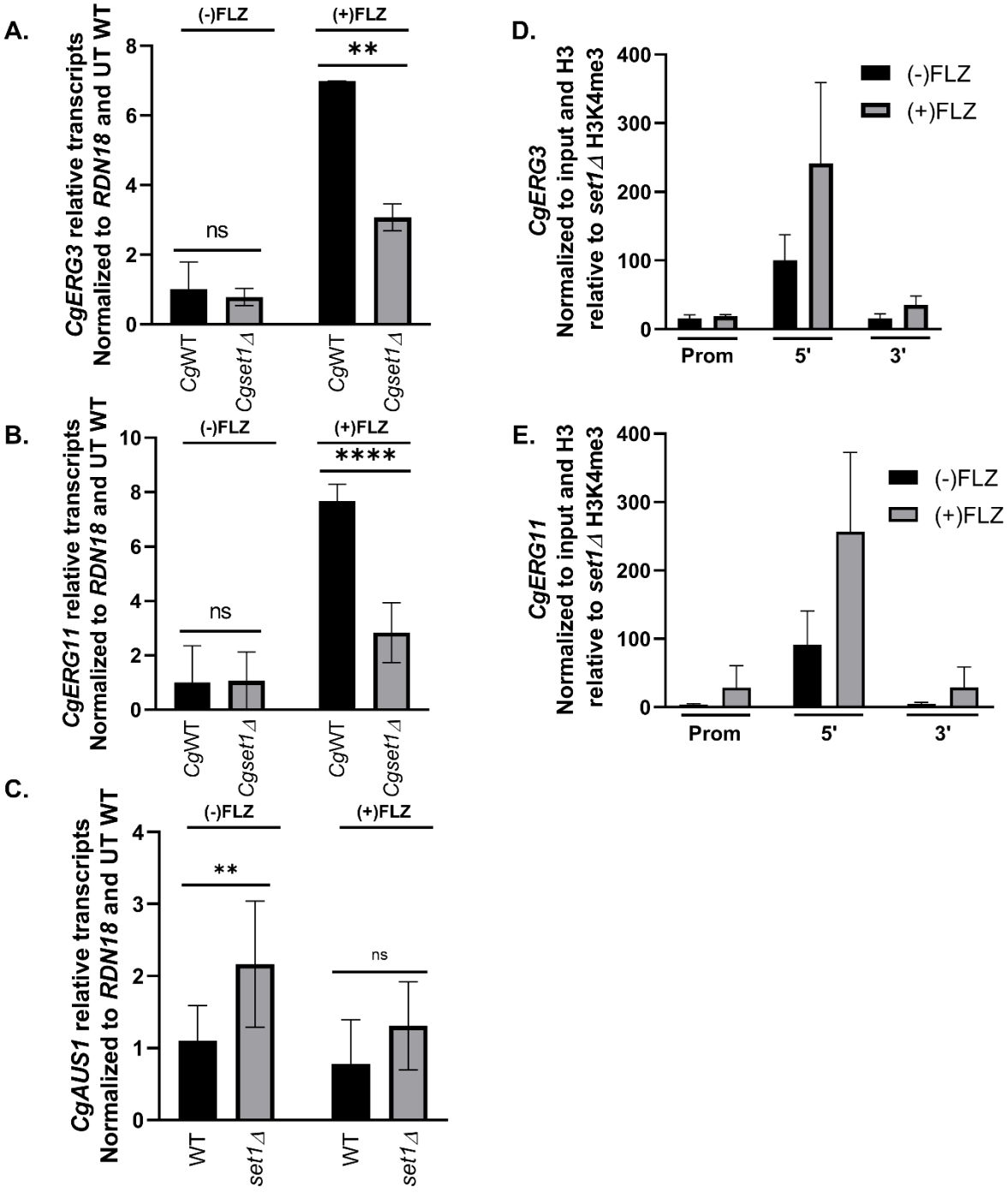

Fig S3. *Histone H3K4 trimethylation is enriched on ERG gene chromatin and Set1-mediated histone H3K4 methyltransferase activity is required for azole induction of ERG genes in saturated cells.* (A and B) Expression of genes was determined in the indicated strains treated with and without 64 µg/ml fluconazole in a saturated culture for 3 hr by qRT-PCR analysis. Gene expression analysis was set relative to the untreated wild-type expression was normalized to *RDN18* mRNA levels. Data were analyzed from ≥ 3 biological replicates with three technical replicates each. (C) Expression of genes was

994 determined in the indicated strains treated with and without 64 µg/ml fluconazole in an
995 exponential culture for 3 hr by qRT-PCR analysis. Gene expression analysis was set
996 relative to the untreated wild-type expression was normalized to *RDN18* mRNA levels.
997 Data were analyzed from ≥ 3 biological replicates with three technical replicates each.
998 (D and E) ChIP analysis of histone H3K4 tri-methylation levels at the promoter, 5', and
999 3' regions of *ERG11* and *ERG3* in a wild-type *C. glabrata* strain with and without 64
1000 µg/mL fluconazole treatment in saturated cell cultures. ChIP analysis was set relative to
1001 a ***set1Δ*** strain and normalized to histone H3 and DNA input levels. Data were analyzed
1002 from 3 biological replicates with three technical replicates each. Statistics were
1003 performed using Graphpad Prism student t-test version 9.2.0. **p<0.05. ****p<0.0001*
1004 *and **p<0.01.* Error bars represent SD.

1005 **Figure S4**

A.

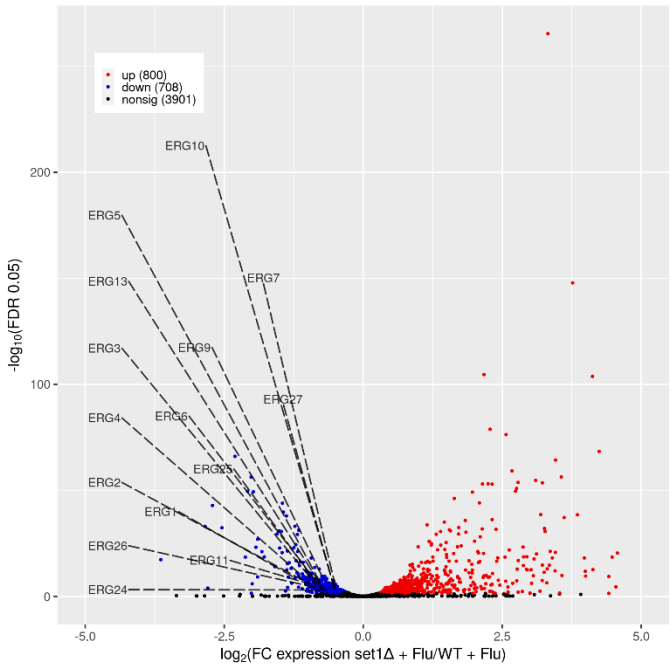

B.

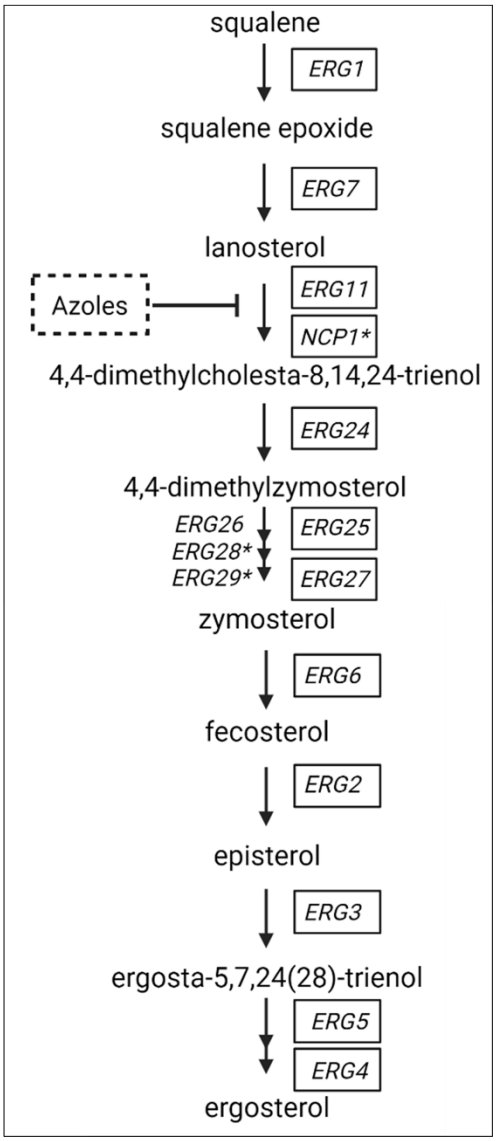

Fig S4. *Genes encoding enzymes of the late ergosterol pathway are down in a set1Δ strain upon azole treatment in C. glabrata.* (A) Volcano plot showing the significance [$-\log_2$ (FDR), *y*-axis] *vs.* the fold change (*x*-axis) of the DEGs identified in the *set1*Δ azole treated samples relative to WT azole treated samples. Genes with significant differential expression (FDR < 0.05) are highlighted in red or blue for up- and downregulated genes, respectively. Down-regulated *ERG* genes are labelled in the plot which include 12 of the *ERG* genes in the late pathway and two *ERG* genes in the early pathway. Black highlighted genes are considered nonsignificant. (B) Depiction of the late ergosterol pathway in *C. glabrata.* Azoles inhibit lanosterol 14-α-demethylase, the enzyme encoded by *ERG11. NCP1** and *ERG28** interact with ergosterol synthesizing enzymes. *ERG29** is a protein of unknown function involved in ergosterol biosynthesis. Loss of *SET1* results in lower transcript levels of 12 of the 12 ergosterol synthesizing enzymes of the late pathway compared to a wild-type strain upon azole treatment. Genes with decreased transcript levels due the loss of *SET1* are surrounded by a solid square.

Supplemental Tables

Table S1.	**Yeast Strains**		
Strains	Genotype	Reference	Strain Name
S. cerevisiae BY4741	*MATα his3Δ leu2Δ0 LYS2 met15Δ0 ura3Δ0*	Open Biosystems	*Sc*WT
Scswd1Δ	*MATα his3Δ leu2Δ0 LYS2 met15Δ0 ura3Δ0 swd1Δ::KanMX*	Open Biosystems	*Scswd1Δ*
Scspp1Δ	*MATα his3Δ leu2Δ0 LYS2 met15Δ0 ura3Δ0 spp1Δ::KanMX*	Open Biosystems	*Scspp1Δ*
Scbre2Δ	*MATα his3Δ leu2Δ0 LYS2 met15Δ0 ura3Δ0 bre2Δ::KanMX*	Open Biosystems	*Scbre2Δ*
SDBY1420	*MATa his3Δ leu2Δ0 LYS2 met15Δ0 ura3Δ0 set1Δ::HphMX*	Zhang et al. Yeast 2017	*Scset1Δ*
SDBY1600	*MATα his3Δ leu2Δ0 LYS2 met15Δ0 ura3Δ0 HHT1::K4R*	This study	*ScH3K4R1*
SDBY1601	*MATα his3Δ leu2Δ0 LYS2 met15Δ0ura3Δ0 HHT1::K4R HHT2::K4R*	This study	*ScH3K4R2*
ATCC 2001 *Cg*WT	*C. glabrata* wild type strain	www.atcc.org	*Cg*WT
SDBY1602	*set1Δ::HphMX*	This study	*Cgset1Δ*
SDBY1603	*swd1Δ::HphMX*	This study	*Cgswd1Δ*
SDBY1604	*spp1Δ::HphMX*	This study	*Cgspp1Δ*
SDBY1605	*bre2Δ::HphMX*	This study	*Cgbre2Δ*
SDBY1606	*pdr1Δ::NatMX*	This study	*Cgpdr1Δ*
ATCC 200989 *Cg*WT	*his3Δ trp1Δ ura3Δ*	www.atcc.org	*Cg*WT

SDBY1607	*his3Δ trp1Δ ura3Δ set1Δ::HphMX*	This study	*Cgset1Δ*

1022

Table S2. Plasmids				
Plasmid	**Inserted Gene**	**Promoter**	**Vector**	**Source**
pGRB2.0	None		pGRB2.0	Zordan et al.
pGRB2.0	*SET1*	*SET1*	pGRB2.0	Zordan et al.
pGRB2.0	*SET1/H1048K*	*SET1*	pGRB2.0	Zordan et al.

1023

Table S3. Primers for qRT-PCR	
Primer Name	**Sequence**
CgRDN18-001F	ACGGAGCCAGCGAGTCTAAC
CgRDN18-002R	CGACGGAGTTTCACAAGATTACC
CgERG3-001F	TGGGAGCACCACGGTCTAAG
CgERG3-002R	CAGTCGGTGAAGAAGATGAAAGTG
CgERG11-001F	GGGTCCAAAGGGTCACGAA
CgERG11-002R	GCAGCTTCAGCGGAAACATC
CgCDR1-001F	GTCTATGGAAGGTGCCGTCAA
CgCDR1-002R	TGAACCAGGTCTACCTAGCACAAC
CgPDR1-001F	TCGGCGAGGGTAAATTCAAC
CgPDR1-002R	CAACTGCGTTTGATTCCTTAAGC
CgSET1-001F	CCAACCAAAGCCGATACTCATC
CgSET1-002R	GCGTTGACTACCGCGAGATT

1024

Table S4. Probe sets for ChIP Analysis	
Probe Name	**Sequence 5'-3'**
ERG11 Promoter	/56-FAM/CCTTGTTCC/ZEN/AACTACAATCGAGTGAGCT/3IABkFQ/ CGAATACGAGGCCATTTGTAAAC CTGTGCTCCCATCTCACTATAAC
ERG11 5'	/56-FAM/TCGTACTTC/ZEN/CAAGCTCTGCCATTGG/3IABkFQ/ GAGTACGTGAAGCTTGGTCTT TGGCAAGGCGACCATAATAG
ERG11 3'	/56-FAM/CGGCATGAC/ZEN/TTAAGCTGGTTGTTTCG/3IABkFQ/ ACGGGATATACGCTGATTCATT AGCAGCAAAGCCCTCTAAA
ERG3 Promoter	/56-FAM/AGCGAGAGC/ZEN/TGCTAGAGCTGAGAA/3IABkFQ/ GAGACTATACGAGTGTGCTCTTTG TCTTCTTCCAGGCCTCATCT
ERG3 5'	/56-FAM/TCGACGACT/ZEN/CGTTGGTCAATGCTT/3IABkFQ/ CGACGATGTGTATGCCAAGA ATGCAGCAGCGTAGAGTTAG
ERG3 3'	/56-FAM/CCAAGAGGT/ZEN/GGAAGGTGACGACAC/3IABkFQ/ AGAAACCGCCGCTTACAT CCGGTGTTTCCTGTCTAGTT

1025

Table S5. qRT-PCR Values

Figure 4A: qRT-PCR

Gene	Strain	Condition	Mean RQ	Standard Deviation	N	P-Value
CgCDR1	*Cg*WT	Untreated	1	0.750623	7	n.s.
CgCDR1	*Cg*WT	(+) fluconazole	4.51	1.071572	7	n.s.
CgCDR1	*Cgset1*Δ	Untreated	1.1	0.972961	7	n.s.
CgCDR1	*Cgset1*Δ	(+) fluconazole	4.04	0.608125	7	n.s.

Figure 4B: qRT-PCR

Gene	Strain	Condition	Mean RQ	Standard Deviation		P-Value
CgPDR1	*Cg*WT	Untreated	1	0.257724	3	n.s.
CgPDR1	*Cg*WT	(+) fluconazole	2.29	0.204429	3	n.s.
CgPDR1	*Cgset1*Δ	Untreated	1.02	0.3498374	3	n.s.
CgPDR1	*Cgset1*Δ	(+) fluconazole	2.29	0.249992	3	n.s.

Figure 5E: qRT-PCR

Gene	Strain	Condition	Mean RQ	Standard Deviation		P-Value
CgERG11	*Cg*WT	Untreated	1	0.32	3	n.s.
CgERG11	*Cg*WT	(+) fluconazole	10.29	0.23	3	n.s.
CgERG11	*Cgset1*Δ	Untreated	1.32	0.65	3	n.s.
CgERG11	*Cgset1*Δ	(+) fluconazole	3.83	0.26	3	<0.0001

Figure 5F: qRT-PCR

Gene	Strain	Condition	Mean RQ	Standard Deviation		P-Value
CgERG3	*Cg*WT	Untreated	1	0.1	3	n.s.
CgERG3	*Cg*WT	(+) fluconazole	3.63	0.69	3	n.s.
CgERG3	*Cgset1*Δ	Untreated	1.14	0.05	3	n.s.
CgERG3	*Cgset1*Δ	(+) fluconazole	0.9	0.18	3	<0.01

Figure 6C: qRT-PCR

Gene	Strain	Condition	Mean RQ	Standard Deviation		P-Value
CgERG11	*Cg*WT+V	Untreated	0.951	0.384	4	n.s.
CgERG11	*Cg*WT+V	(+) fluconazole	6.791	1.988	4	n.s.
CgERG11	*Cgset1*Δ+V	Untreated	1.342	0.549	4	n.s.
CgERG11	*Cgset1*Δ+V	(+) fluconazole	2.603	1.043	4	<0.01
CgERG11	*Cgset1Δ/SET1*	Untreated	1.227	0.631	4	n.s.
CgERG11	*Cgset1Δ/SET1*	(+) fluconazole	6.438	2.783	4	n.s.
CgERG11	*Cgset1Δ/H1048K*	Untreated	1.346	0.429	4	n.s.
CgERG11	*Cgset1Δ/H1048K*	(+) fluconazole	3.370	0.870	4	<0.05

Figure 6D: qRT-PCR

Gene	Strain	Condition	Mean RQ	Standard Deviation		P-Value
CgERG3	*Cg*WT+V	Untreated	1.266	1.138	4	n.s.
CgERG3	*Cg*WT+V	(+) fluconazole	5.686	2.144	4	n.s.
CgERG3	*Cgset1*Δ+V	Untreated	0.814	0.345	4	n.s.
CgERG3	*Cgset1*Δ*I*+V	(+) fluconazole	1.512	0.429	4	n.s.
CgERG3	*Cgset1Δ/SET1*	Untreated	1.034	0.64	4	n.s.
CgERG3	*Cgset1Δ/SET1*	(+) fluconazole	7.518	4.232	4	<0.001

CgERG3	*Cgset1Δ/H1048K*	Untreated	0.888	0.206	4	n.s.
CgERG3	*Cgset1Δ/H1048K*	(+) fluconazole	2.357	0.54	4	<0.05

Figure 6A: ChIP qRT-PCR

Gene	Strain	Condition	Mean RQ	Standard Deviation		P-Value
CgERG11	*Cg*WT promoter	Untreated	11.24	5.568	3	n.s.
CgERG11	*Cg*WT promoter	(+) fluconazole	22.138	12.012	3	n.s.
CgERG11	*Cg*WT 5'	Untreated	62.531	1.452	3	n.s.
CgERG11	*Cg*WT 5'	(+) fluconazole	133.274	20.388	3	<0.001
CgERG11	CgWT 3'	Untreated	11.412	3.193	3	n.s.
CgERG11	CgWT 3'	(+) fluconazole	26.019	7.85	3	<0.05

Figure 6B: ChIP qRT-PCR

Gene	Strain	Condition	Mean RQ	Standard Deviation		P-Value
CgERG3	*Cg*WT	Untreated	35.768	18.274	3	n.s.
CgERG3	*Cg*WT	(+) fluconazole	57.996	35.319	3	n.s.
CgERG3	*Cg*WT 5'	Untreated	145.877	42.565	3	n.s.
CgERG3	*Cg*WT 5'	(+) fluconazole	281.392	69.117	3	<0.05
CgERG3	CgWT 3'	Untreated	50.262	13.737	3	n.s.
CgERG3	CgWT 3'	(+) fluconazole	133.95	59.062	3	n.s.

1026

1027